SYNTHESIS AND ANTIBACTERIAL PROPERTIES OF SELENIUM BASED NANOPARTICLES MADE BY BACTERIA

A Thesis Presented
by
Lorena Baranda Pellejero
to
The Department of
Chemical Engineering

In partial fulfillment of the
requirements
For the degree of

Master in Nanoscience,
Materials and Processes

In the field of
Chemical Engineering

JULY 30, 2018

NORTHEASTERN UNIVERSITY
BOSTON, MASSACHUSETTS
UNIVERSITAT ROVIRA I VIRGILI
TARRAGONA, SPAIN

ACKNOWLEDGEMENTS

I would like to thank Professor Thomas Webster for the opportunity he gave me to develop my master project in his lab. I am grateful to him for his guidance and for encouraging me to attend to conferences and contests to make the most of my research experience here. Thanks to David Medina who have read through this thesis and for teaching me the lab techniques.

I would like to express my gratitude to Northeastern University for providing all the laboratory equipment to make this research and all the ongoing projects in this Nanomedicine lab possible. Thanks to every faculty member and staff from the Department of Chemical Engineering for helping me with all the procedures needed to accomplish this research.

Thanks to University Rovira I Virgili in Tarragona (Spain), and specially to the master's coordinator Jordi Riu, for all the effort and work that involves making this program possible.

Thanks to William Fowle for his expertise and technical assistance in electron microscopy and also to the Center for Nanoscale Systems at Harvard University for their XPS instrumentation.

I would also wish to express my gratitude to Prof. Ryan Koppes and Prof. Hicham Fenniri, as they kindly agreed to be part of my committee for the defense of my master's thesis.

My most sincere thanks to all my lab mates, who have been always there, willing to help and give advice. Specially, I must highlight three persons that have been indispensable to achieve my work here, not only for their valuable suggestions, support and patience, but also for being able to turn this internship into an unforgettable experience. Thanks Claudia, Miguel and Caterina.

Finally, but not least, I would like to mention my family, specially my parents, to which I do not have proper words to describe how thankful I am for their love and support throughout my entire life. Without them, this research nor the completion of my master would have not been possible. Thanks for always supporting my dreams and aspirations and for all you have done for me.

TABLE OF CONTENTS

1. INTRODUCTION

Bacterial infections are considered one of the most significant problems currently facing the healthcare system. One of the main reasons is the extreme ease with which bacteria can be acquired in environments and procedures such as medical interventions, and these are able to cause serious illnesses if not treated efficiently [1]. The second reason is related to the appearance of various mutations in the bacteria that lead to their resistance towards current treatments [2].

Current treatments to fight bacterial infections are comprised of antibiotic regimens, also known as antimicrobial agents, which have been used for 70 years to treat patients [3]. However, their effect is now being limited by the appearance of resistive bacterial mutations, which are produced mainly due to the natural origin of antibiotics and the wide and intensive use of these drugs by humans [4]. First, the fact that most antimicrobial agents are naturally-produced molecules allows bacteria to develop mechanisms to overcome their action and survive, known as antimicrobial resistance (AMR) [5]. Second, there is a significant human contribution to the evolution of AMR due to the over-prescription of antibiotics, public misconceptions, and their misuse by the food industry [6]. The consequences of this, for instance, can be exemplified by the case of methicillin-resistant *Staphylococcus aureus* (MRSA). It is a specific strain of *Staphylococcus aureus* (*S. aureus*) that eventually became resistant to methicillin, the common type of antibiotic used to treat *S. aureus* [7]. In *Figure 1,* several antibiotics to which bacteria have develop resistance within time is listed. According to the Centers for Disease Control and Prevention (CDC), 80,461 severe MRSA infections and 11,285 related deaths were reported in 2011, showcasing the serious threat of this microorganism to human health. Moreover, a much higher number of minor infections occurred within both the community and healthcare environments [8].

According to the World Health Organization (WHO), AMR is causing over 150,000 deaths per year in hospitals around the planet [9], resulting in a cost for the U.S. health care system of over $20 billion each year [10]. By 2050, it is expected that there will be more deaths caused by bacterial infections than for cancer [11]. Therefore, there is an urgent need for novel treatments against bacteria to avoid the use of antibiotics.

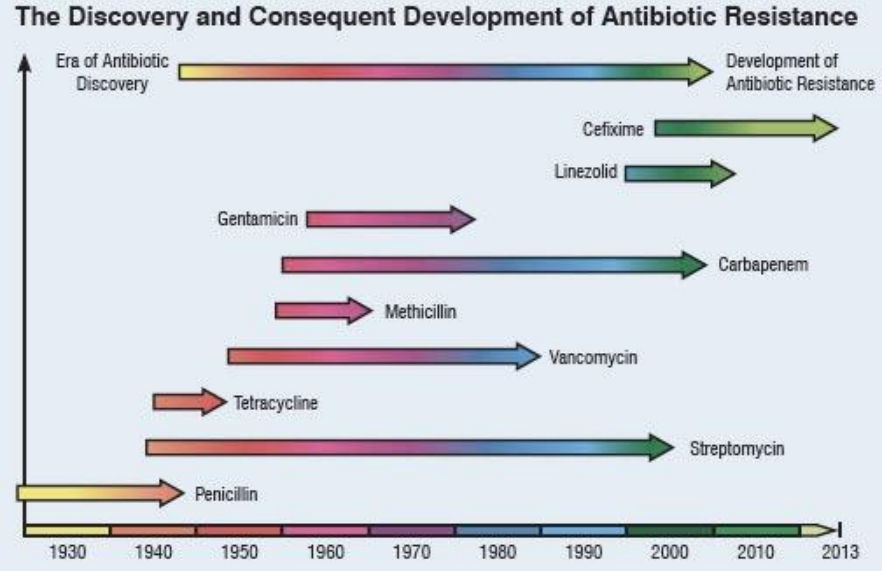

Figure 1. **Timeline of antibiotic discovery and the development of antibiotic resistance**. Image from Nanowerk, Nanotechnology solutions to combat superbugs. https://www.nanowerk.com/spotlight/spotid=32188.php

Recent developments in nanotechnology have been proven to show high potential as a long-term solution to the ever-growing problem of AMR. The properties of materials change drastically when their dimensions are extremely reduced, reaching the nanoscale. Nanomaterials, which are considered to have at least one dimension under 100 nm, are characteristic due to their high surface area-to-volume ratio and the appearance of discrete electronic states at these extremely low dimensions, both being responsible for their novel physical, chemical and biological properties [12, 13]. Materials such as nanoparticles (NPs) offer a wide range of possibilities for biomedical applications, as they can act as carriers for drugs, preventing them from degradation, be functionalized for targeting a specific site within the body, or act as therapeutic agents themselves,

due to the increased reactivity produced by their high surface area [14-16]. Regarding their use as drug carriers, NPs can be constructed to possess different properties and characteristics for the best delivery or encapsulation of the therapeutic agent. Researchers from the California Nanosystems Institute devised a novel approach to treat cancer by delivering camptothecin and other water insoluble drugs directly to cancer cells by using silica-based NPs [17]. Moreover, the modification of the NP's surface to direct them to a specific site and/or improve the cell interaction properties were performed. Based on knowledge of markers and proteins expressed on cancer cells, N. H. Ellah et al. introduced variable bioactive molecules to NPs to improve the specific interaction between the nanoparticle and the cell [18]. Finally, NPs can be used as the direct therapy, rather than a drug carrier. The most common type of NPs used in this approach are metal and metal oxide-based NPs. In 2007, Tian et al. demonstrated that the delivery of silver NPs promoted wound healing and reduced scar appearance in a dose-dependent manner in mice [19].

One of the most common types of NPs used to treat diseases are those composed of metals [20]. The therapeutic properties of metals have been applied since ancient times. Especially, the antimicrobial properties of metals such silver and copper have been known for a long time against a wide range of Gram-positive and Gram-negative bacteria [21]. When these metals present dimensions at the nanoscale, they experience a higher interaction, leading to increased antibacterial efficiency [22].

To date, many different types of metallic NPs demonstrated anticancer and antibacterial properties [23, 24]. Materials including silver [25, 26], gold [27], titanium dioxide [28], zinc oxide [29], iron oxide [30], silica [31], and carbon [32, 33] have presented therapeutic properties. For instance, silver NPs, prepared by a reduction method, have been shown to be toxic to both *Pseudomonas aeruginosa* (*P. aeruginosa*) and *Escherichia coli* (*E. coli*) [34]. Moreover, iron oxide NPs

synthesized via a one-step solvothermal method were an effective antibacterial agent against both Gram-positive and Gram-negative bacteria [35].

The small size, together with the high reactivity of NPs, make it possible for them to directly interact with microorganisms in an effective manner, decreasing their survival rate [22]. L.S. Reddy et al. showcased the ability of zinc oxide NPs to rupture the bacterial cell wall and bind to intracellular material, clearly inhibiting bacterial growth [36].

There are mainly two types of mechanisms through which NPs attack pathogens. The first is thought to be related to the generation of reactive oxygen species (ROS) [37]. The cell wall is believed to be damaged by ROS oxidation, being later destroyed and all the cellular content released into the extracellular media. These ROS are also believed to produce damage in proteins, altering their regulation, and also in the DNA content within the cell [37]. The second type of mechanism involves the release of metal ions from the nanostructures, causing an antibacterial effect over the infection. These ions are normally adsorbed by the cell membrane, directly interacting with internal components [38].

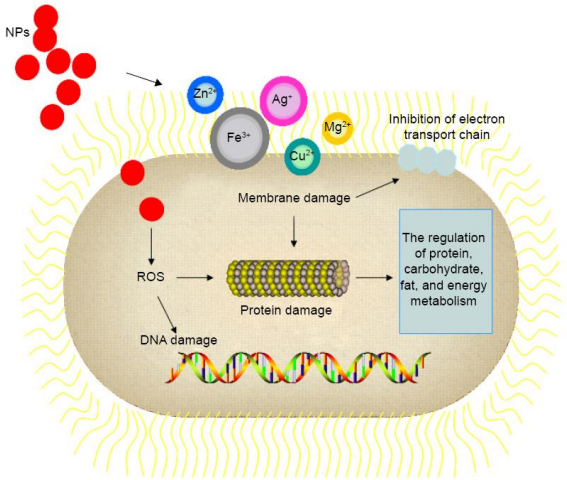

Figure 2. **Mechanisms of NP action in bacteria cells**. Image from "The antimicrobial activity of NP: present situation and prospects for the future" Wang LL, Hu C, Shao LQ. Dovepress, Volume 2017:12 Pages 1227—1249

The aspect that most determines the properties and characteristics of NPs is how they are produced. Conventional synthetic routes followed to obtain metallic NPs are usually based on physical or

chemical methods. The former involves methods such as laser ablation [39], ultraviolet radiation [40], and hydrothermal techniques [41] whereas the latter consists of catalytic reduction and precipitation, among others [42]. These methods are well studied, and numerous established protocols have been defined. Nonetheless, they are extremely costly and involve the use and production of toxic and hazardous chemicals, thus being a potential environmental threat. Moreover, reaction conditions are usually harsh, needing high temperatures and pressures for efficient synthesis [43]. Aggregation of recently synthesized NPs can also occur [44]. Furthermore, NPs obtained by physico-chemical methods need to be functionalized in order to be biocompatible, which is an essential requirement for use in biomedical applications [45].

Thus, there is a need to develop new methods for NP synthesis that avoid the aforementioned drawbacks. Fortunately, green chemistry has provided sustainable methods that reduce or eliminate the use or generation of hazardous substances in the production of these materials. It takes advantage of nature, specifically of biological systems, which are able to synthesize nanomaterials in an inherently non-toxic way [46]. It is possible to use any natural compound such as microorganisms (e.g. bacteria, plants, yeast) or any material composed of biomolecules (e.g. food extracts, waste material) to accomplish a natural synthetic method [47, 48].

There is a specific type of green synthesis that utilizes bacteria to achieve a desired nanomaterial, known as "bacteriogenic synthesis" [49]. Bacteria produce a detoxification process in presence of metal ions, which is a remarkable defense mechanism to cope with the toxicity and stress induced by these ions [50]. The bacteria are then able to reduce and precipitate these metallic ions into NPs, becoming one of the best candidates for NP synthesis. A wide number of well-known types of bacteria has been reported to synthesize NPs. Species like *P. aeruginosa*, *E. coli*, *S. aureus*, *Bacillus cereus* (*B. cereus*) and *Filamentous cyanobacteria* (*F. cyanobacteria*), and others have been used to produce selenium, gold and silver NPs, among others [51-54].

Specially, bacteriogenic synthetic routes for obtaining selenium NPs (Se-NPs) were first studied by Gerard et. al in 1974, obtaining Se-NPs from *E. coli* [55]. These NPs can be synthesized extracellularly, intracellularly or on the cell membrane. Among them, the one that presents more advantages is extracellular synthesis, as the isolation of NPs is easier as if they were formed inside the cell [56]. The enzymes responsible for the reduction reaction are reductases such as selenate, nitrite and sulphite, depending on the microorganism [57]. Many Gram-positive and Gram-negative bacteria have been reported to reduce selenium oxyanions into elemental selenium under aerobic and anaerobic conditions [58]. However, the antimicrobial properties of these bacteriogenic Se-NPs have been barely explored.

Besides the widely used biogenic synthesis for monometallic NPs, there are few examples that apply this approach for obtaining bimetallic NPs (BNPs). Most of them utilized plant-mediated synthesis, using leaf extracts as reducing and capping agents. S. Mondal et al. demonstrated for the first time the superb efficiency of aqueous extract of dried leaves of mahogany in the rapid synthesis of stable Au/Ag BNPs [59]. Likewise, R. Dobrucka et al. reported the synthesis of core-shell Cu@Pt NPs by *Agrimoniae herba* extract, a medicinal plant rich in biologically active substances [60]. These nanostructures hold numerous applications including electrical, optical, catalytic and biomedical. Specifically, BNPs such as cadmium selenide (CdSe) and zinc selenide (ZnSe) present semiconductor behavior due to the synergy of both elements, which confer them new electronic properties. They have been synthesized by several chemical and physical methods [61-63], however, the capabilities of bacteria to synthesize them establishes a complete new field. One very interesting advantage of biogenically synthesized NPs is the presence of a coating surrounding their surface, which is composed of biological molecules, such as lipids, proteins and hydrocarbons, coming from the bacteria [64, 65]. This prevents the aggregation of the NPs and

enhances their biocompatibility, thus avoiding the additional functionalization step needed in physico-chemical routes [66, 67].

Hence, the aim of the present thesis is to explore bacteriogenic synthetic routes for the generation of selenium-based metallic NPs to be further applied in bacterial treatments and biocompatibility assays. The present work is divided into two main objectives: in the first, selenium Se and CdSe metallic NPs made by *S. aureus* and *E. coli* were synthesized and their antibacterial activity against Gram-positive and Gram-negative bacteria studied. In the second objective, a novel route for the treatment of *Helicobacter pylori* (*H. pylori*) infection by using Se-NPs was studied. A nanometric trojan horse approach was taken, in which bacteria were treated with the NPs that they themselves created. The size, shape and charge of all the synthesized NPs were characterized by transmission electron microscopy (TEM) and dynamic light scattering (DLS) and their composition by energy-dispersive X-ray spectroscopy (EDX) and X-ray photoelectron spectroscopy (XPS). After synthesis and characterization, the antibacterial properties were tested by bacterial growth curve analysis and colony-forming unit assays. Finally, the biocompatibility of the metallic NPs was explored by studying their cytotoxic effects on healthy human dermal fibroblasts (HDF).

2. MATERIALS AND METHODS

2.1. Materials

E. coli (strain K-12 HB101; Bio-Rad, Hercules, CA) and *S. aureus* subsp. *aureus Rosenbach* (ATCC 12600™) were used to synthesize selenium-based metallic NPs. Luria-Bertani Broth (LB, 10 g/L Tryptone, 10 g/L sodium chloride, 5 g/L yeast extract) was purchased from Sigma-Aldrich (St Louis, MO, US) and was used for the incubation of *E. coli* and *S. aureus* bacteria. *H. pylori* (ATCC® 43504™) was used to synthesize SeNPs. Tryptic Soy Broth (TSB, 2.5 g/L dipotassium hydrogen phosphate, 2.5 g/L glucose, 5 g/L sodium chloride, 3 g/L soya peptone) was purchased from Sigma-Aldrich and used for *H. pylori* incubation.

For the NP synthesis and antibacterial assays, sodium selenite (Na_2SeO_3), cadmium chloride ($CdCl_2$), zinc nitrate hexahydrate ($Zn(NO_3)_2.(H_2O)_6$), sodium chloride (NaCl), tris(hydroxymethyl)aminomethane buffer (Tris/HCl), phosphate-buffered saline (PBS), agar powder and non-tissue-treated 96-well plates were all purchased from Sigma-Aldrich.

For the cytotoxicity assay, human dermal fibroblasts were purchased from the American Type Culture Collection (ATCC® PCS-201-012™; Manassas, VA, US). Dulbecco's Modified Eagle's Medium (DMEM) and penicillin/streptomycin were purchased from Thermo Fisher Scientific. Fetal bovine serum was purchased from the American Type Culture Collection (ATCC 30–2020™; Manassas, VA). Poly-d-lysine vented cap flask, tissue-treated 96 well plates and trypsin were purchased from Sigma-Aldrich. For the MTS assay, the kit used was a Promega CellTiter 96 Aqueous One solution cell-proliferation assay purchased from Thermo Fisher Scientific.

2.2. Instruments and characterization

Cultures were incubated in a MaxQ4000 from Thermo Scientific. Centrifugation of samples was accomplished using both an Eppendorf™ Model 5430 Microcentrifuge and Eppendorf Model Centrifuge 5804R, refrigerated, with Rotor A-4–44 incl. adapters for 15/50 mL conical tubes, keypad, 230 V/ 50260 Hz. A FreeZone Plus 2.5 Liter Cascade Console Freeze Dry System was used to completely dehydrate the samples, obtaining a fine powder. Morphological characterization of the metallic NPs was accomplished by TEM using a JEM-1010 TEM (JEOL USA Inc., MA). To prepare samples for TEM imaging, particles were dried on 300-mesh copper-coated carbon grids (Electron Microscopy Sciences, Hatfield, PA). The diameter, charge and mobility of the synthesized NPs were studied by DLS using a 90Plus Particle Size Analyzer from Brookhaven Instruments Corporation. The samples were analyzed at a concentration of 1 mg/mL NPs in Milli-Q water. The composition of the NPs was analyzed by SEM coupled to an EDX instrument using a SEM HitachiS-4800 equipped with EDX analysis. The procedure followed for sample preparation was the same that the one used for TEM. XPS analysis was also performed on the NPs in powder form to analyze their composition, using a Thermo Scientific K-Alpha+ XPS System. The sample preparation for XPS required the NP powder to be on carbon tape stuck onto aluminum foil and loaded into the XPS holder. A SpectraMax M3 spectrophotometer (Molecular Devices, Sunnyvale, CA) was used to measure the optical density of the bacterial cultures. Growth curve assays were performed in a plate reader, SpectraMaxV R ParadigmV R Multi-Mode Detection Platform.

2.3. Bacterial culture

For the agar plate culture preparation, 0.5 mL of the cell vial was added to 5 mL of LB medium for *E. coli* and *S. aureus* and to TSB medium for *H. pylori* and incubated overnight to allow bacteria to reach the stationary growth phase. A solution of 10^5 cells/mL was prepared, and 100 µL was taken and spread into an agar plate with an L-shaped cell spreader. It was left in the incubator for 10-12 h to allow the growth of colonies and then stored at -4°C.

For the inoculum preparation, a loop of the agar plate culture was inoculated into 40 mL of the respective sterile media in a 50 mL conical centrifuge tube and incubated at 37°C, 200 rpm for 16 h. *E. coli* and *S. aureus* were incubated in LB medium, whereas *H. pylori* was incubated in TSB medium. After this time, two different methods were followed, depending on the desired starting concentration of bacteria:

- To start with a relatively low concentration of bacteria, the cells were harvested by centrifugation at 5000 rpm for 10 min. Then, the supernatant was collected and transferred into a 50 mL Falcon tube, and the pellet was discarded. The optical density of the supernatant phase was measured using a spectrophotometer at 600 nm (OD_{600}), to estimate the number of bacterial cells per mL for further experiments. Values around 0.05 were expected from both bacteria, corresponding to a concentration of approximately 10^8 cells/mL.
- To start with the maximum concentration of bacteria, the bacterial culture after the incubation time was directly used for further experiments. Values around 0.42 were normally obtained, corresponding to a concentration of around 10^9 cells/mL.

2.4. Synthesis of NPs

- **Synthesis of selenium-based NPs by *E. coli* and *S. aureus***

For the NPs synthesis, an aqueous solution of 2 mM sodium selenite (Na_2SeO_3) was added to a 40 mL isolated supernatant following the procedure described in the "Bacterial culture" section, starting with an approximate bacterial concentration of 10^8 cells/mL. Once bacteria were inoculated with the metallic salt, they were kept in a shaking incubator at 37°C, 200 rpm for 2 h. After this time, a second inoculation with metal was performed by adding 0.75 mM of cadmium chloride and zinc nitrate hexahydrate for the obtention of CdSe- and SeNPs, respectively. Bacteria were cultivated in the dark for 24 h at 37°C and 200 rpm.

The same procedure as the one previously described was followed starting with a bacterial concentration of 10^9 cells/mL.

- **Synthesis of Se-NPs by *H. pylori***

For the production of Se-NPs, an aqueous solution of sodium selenite (Na_2SeO_3) at different concentrations (1, 2, 5 mM) was added to the 40 mL supernatant previously treated as described in the "Bacterial inoculum preparation" section. The solution was incubated while shaking at 37°C, 200 rpm for 72 hours to achieve biosynthesis. After the reaction, a change of color from yellowish was observed, which is the color of LB media, to orange-red, indicating the reduction of SeO_2^{-3} to elemental selenium (Se^0).

2.5. Purification of NPs

For the purification of NPs, the samples containing bacteria and NPs were centrifuged at 7500 rpm for 10 min. The supernatant was removed, and the pellet was washed twice with a 0.9% NaCl solution and finally with 15 mL of a Tris/HCl buffer solution to completely stop bacterial growth. The solutions were sonicated for 15 min to allow for disruption of the bacterial membranes followed by the release of the NPs. After sonication, they were centrifuged again at 7500 rpm for 10 min and re-suspended in 10 mL of sterile Milli-Q water.

After purification, these solutions were place in a freezer at -80°C for 4 h. Then, the solutions were placed in a freeze-dryer. The top of each tube was replaced for a piece of holey parafilm beforehand in order to allow the release of the solvent during the freeze-drying step. The samples were kept overnight until all the solvent was removed. The obtained powder was first weighed and then resuspended in Milli-Q water to achieve the desired concentration for further experiments.

All sterile liquids (LB, TSB, Milli-Q water, 0.9% NaCl, Tris/HCl buffer, PBS) were autoclaved under a standard sterilization procedure that subjects the load to high-pressure saturated steam at 121°C for 110 min.

2.6. Growth curve assay

For the growth curve assay, two main studies were accomplished: one studying the influence of the metallic salt in bacterial growth and the other testing the antimicrobial activity of the NPs. For the experiment, different concentrations of the desired agent to be tested, either metallic salt or NPs, were mixed with media (LB or TSB) together with bacteria at a concentration of 10^6 colony forming units per milliliter (CFU/mL) in a non-tissue-treated 96-well plate. Once the plate was prepared, the absorbance of all the samples was measured at 600 nm on an absorbance plate reader

(SpectraMax Paradigm Multi-Mode Detection Platform) every 2 min for 24 h to determine bacterial growth. Curves were fitted using the Gompertz model.

- **Study of the influence of different selenium metallic salts on *H. pylori* growth**

In order to determine the influence of the presence of metallic salt on bacterial growth, several concentrations (5, 4, 3, 2 and 0.1 mM) of different Se metallic salts (Na_2SeO_3, Na_2SeO_4, H_2SeO_3 and $HNaO_3Se$) were mixed with 100 µL of bacteria at a concentration of 10^6 CFU/mL in TSB medium in a non-tissue-treated 96-well plate. The absorbance of all samples was measured at 600 nm on an absorbance plate reader every 2 min for 24 h.

- **Antimicrobial activity of Se-NPs in *H. pylori***

In this study, the influence of three different types of SeNPs, synthesized by adding 1, 2 and 5 mM Na_2SeO_3, were tested against *H. pylori*. Different concentrations of NPs (100, 75, 50, 25, 10 and 5 µg/mL) and the control were mixed with 100 µL of bacteria at a concentration of 10^6 CFU/mL in TSB medium in a non-tissue-treated 96-well plate. Negative controls containing only NPs and medium were used to determine the absorbance caused by the NPs. The absorbance of all samples was measured at 600 nm on an absorbance plate reader every 2 min for 24 h.

2.7. Colony forming units assay

This assay was performed in order to determine the antimicrobial activity of the NPs. Bacteria at a concentration of 10^5 CFU/mL were seeded in a 96-well plate together with different concentrations of NPs (75, 50, 25, 10 and 5 µg/mL) and a bacterial control without NPs. The final volume per well was 200 µL. The plate was placed for 8 h inside a static incubator at 37°C. Then, all samples from the 96-well plate were diluted with PBS in a series of vials to 100×, 100,000×, and 1,000,000×. Three 10 µL drops of each dilution were placed in a TSB-Agar plate and incubated

for 10 h inside the incubator at 37°C. After this time, the colonies were formed and inspected in order to find the dilution that provided the colonies with the best conditions (countable and same diameter of CFU). These colonies would be the ones selected to be counted. For this experiment, Se and CdSe NPs were tested against *E. coli* and *S. aureus* and Se-NPs were tested against *H. pylori*.

2.8. In vitro cytotoxicity assay

Cytotoxicity assays were performed with primary human dermal fibroblasts (HDF). First, they were cultured in complete media (DMEM with 10% fetal bovine serum and 1% penicillin–streptomycin) separately in a flask at 37°C in a humidified incubator with 5% carbon dioxide (CO_2). Then, cells were seeded in a 96-well plate at 5,000 cells/well in 100 µL of cell medium and incubated for 24 h at 37°C in a 5% CO_2 humidified atmosphere. The culture medium was then replaced with 100 µL of freshly prepared culture medium containing different concentrations of NPs (75, 50, 25, 10 and 5 µg/mL). The plate was cultivated again for 24 h in the same environmental conditions as before. The culture media was removed again and replaced with 100 µL of an MTS solution prepared at a mixing ratio of 1:5 of MTS:DMEM. The well plate was then cultivated for 3 h to allow for a color change. Then, the absorbance was measured at 490 nm under an absorbance plate reader (SpectraMax) for cell viability after exposure of cells to the NPs. Cell viability was calculated by dividing the average absorbance obtained for each sample by the one achieved by the control sample, and then multiplied by 100. Controls containing cells and media, and just media, were also included in the 96-well plate to identify the normal growth of cells without NPs and to determine the absorbance of the media.

2.9. Statistical analysis

Each experiment was performed at least three times to ensure the reliability of the results. Data are presented as mean with standard error of the mean, and two-tailed Student's T-tests were used to evaluate the differences between means, with an alpha value of $P<0.1$ being considered statistically significant.

3. RESULTS AND DISCUSSION

3.1. Objective I: Synthesis of selenium based metallic NPs by *E. coli* and *S. aureus.*

3.1.1. Synthesis

With the aim of exploring the synthesis capabilities of *S. aureus* and *E. coli* to produce selenium-based NPs, two synthesis methods were followed by adding different metallic salts: (1) Na_2SeO_3 plus $CdCl_2$ and (2) Na_2SeO_3 plus $Zn(NO_3)_2•(H_2O)_6$. The nature of the obtained NPs determined the ability of the bacteria to reduce these salts. Starting with an initial bacterial concentration of 10^8 cells/mL, a final concentration of 2 mM Na_2SeO_3 was added to cultures corresponding to *E. coli* and *S. aureus* and after two hours, 0.75 mM of either $CdCl_2$ or $Zn(NO_3)_2•(H_2O)_6$ were added. After the reaction, the culture acquired a reddish color for the tubes in which the zinc salt was added and a much lighter red color for the ones corresponding to the cadmium salt, as it can be seen in *Figure 3*. These changes in color provided evidence of the production of NPs. It should be pointed out that for the case of NPs synthesized by *S. aureus*, the culture showed a slightly darker color than those synthesized by *E. coli*, which suggests that *S. aureus* were able to produce NPs with a higher diameter and/or in a higher yield. The color of the reaction of NPs produced can be compared to the one corresponding to the control, which showed the normal growth of the bacteria, presenting a cloudy yellow color.

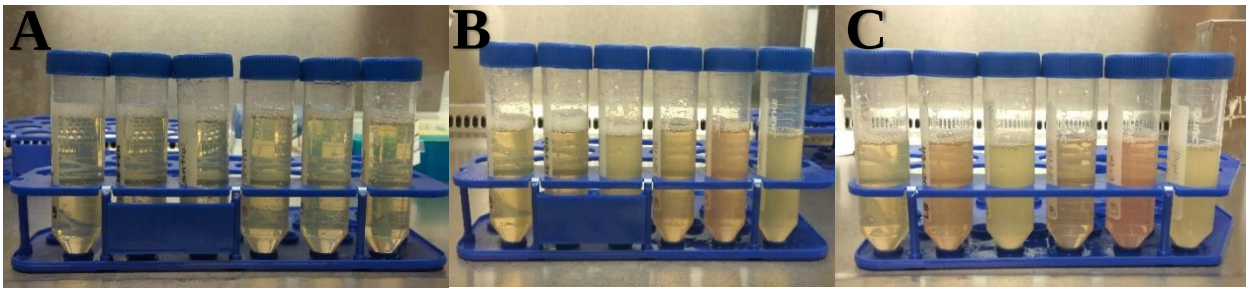

Figure 3. **Color change during the synthesis of NPs**. From left to right, falcon tubes corresponding to the addition of $CdCl_2$, $Zn(NO_3)_2$ and control for *E. coli* and $CdCl_2$, $Zn(NO_3)_2$ and control for *S. aureus*. Color before metallic inoculation (**A**), after 9 h of Na_2SeO_3 addition (**B**) and after 24 h (**C**).

These changes in color revealed the mechanism of production of NPs by bacteria, which cope with the toxicity of the metallic salts added by reducing them to the form of NPs.

Metal ions, in this case SeO_3^{2-} and Cd^{2+}, are normally first trapped on the surface or inside of the microbial cell and then reduced into NPs by bacterial enzymes, known as the "detoxification process" [68]. In some microorganisms, the enzymes that intervene in the SeO_3^{2-}reduction reaction are respiratory reductases of anaerobic respiration, such as nitrite reductase, sulfite reductase and fumarate reductase [57]. Moreover, disulfide reductases play a role in the reduction of cadmium chloride [69]. However, the mechanism used for metal ion reduction can vary between bacterial species.

This synthesis, which is validated in the following "characterization" section, produced CdSe and Se NPs upon first adding Na_2SeO_3, followed by $CdCl_2$ and $Zn(NO_3)_2•(H_2O)_6$ after two hours, respectively. In the first case, CdSe-NPs were formed, demonstrating the ability of bacteria to reduce both selenium and cadmium metallic salts to the corresponding metals at oxidation state zero. In contrast, for the case of the addition of the zinc salt, bacteria were not able to reduce zinc ions, evidenced by the formation of purely Se-NPs. In other words, there was no zinc present in the NPs, suggesting that it remained in its ionic form during the reaction.

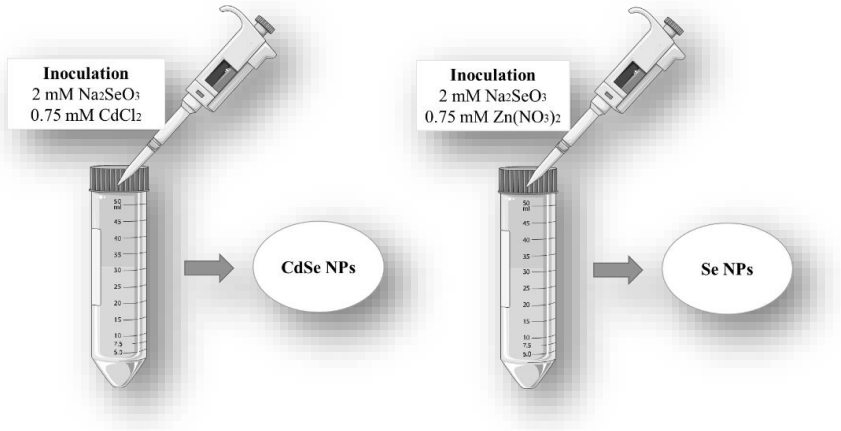

Figure 4. Graphical image showing the results of the synthesis depending on the nature of the second metallic salt added.

Finally, upon comparison with the control samples (salts and media), the dark red color of the samples containing bacteria indicated that the ion reduction was accomplished by enzymes coming from the bacteria and not compounds contained in the medium. Under reaction conditions in the medium phase, the reduction of metal ions did not occur as evidenced by a lack of red-colored precipitation.

3.1.2. Characterization

NPs were named with the following nomenclature: (i) CdSe-NPs synthesized by *E. coli* as EC-CdSeNPs, (ii) Se-NPs synthesized by *E. coli* as EC-SeNPs, (iii) CdSe-NPs synthesized by *S. aureus* as SA-CdSeNPs, and (iv) Se-NPs synthesized by *S. aureus* as SA-SeNPs (Table I).

The morphology of the synthesized NPs was studied by TEM (*Figure 5*). Metallic NPs made by each bacterium showed a uniform spherical morphology. From the TEM images, spherical, metallic-like NPs together with cellular debris can be inferred. Although the purification process was aimed to remove as much cellular material as possible via chemical washes and sonication, it needs to be further improved. The sizes of the synthesized NPs ranged between 150 and 230 nm. One of the most important aspects that can be observed from this characterization is the presence of a natural coating surrounding the NPs, which is a result of the bacteriogenic synthesis. It can be perceived by the difference in contrast between the biomolecules that form the coating (composed by light elements such as carbon and sulfur, among others) and the metallic core, which is dark in comparison as metals do not allow many electrons to be transmitted. This coating is mainly made of biomolecules coming from the bacteria, such as lipids and proteins. It prevents the NPs from aggregation and, it is also hypothesized that it might improve the antibacterial activity and the biocompatibility.

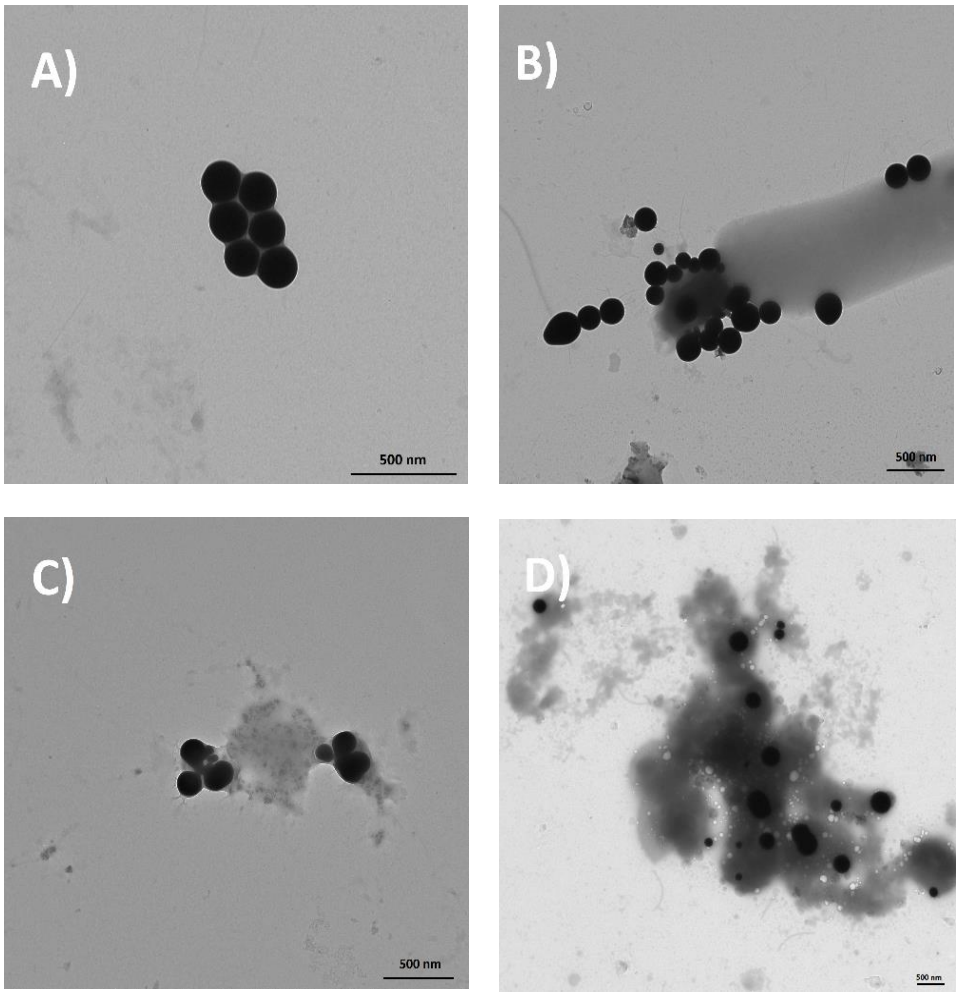

Figure 5. TEM images of the synthesized metallic NPs. From left to right EC-CdSe (A), EC-Se (B), SA-CdSe (C) and SA-Se (D) NPs.

The NP size distribution, Z-potential and mobility of all the synthesized NPs were characterized by DLS measurements (*Table 1*). Results from the NP diameter showed a higher diameter for the synthesized Se-NPs compared to the bimetallic CdSe-NPs, for both types of bacterium, *E. coli* and *S. aureus*. The NP size distribution was plotted for the particular case of Se-NPs made by both *E. coli* and *S. aureus* in *Figure 6*. It can be observed that the NP size distribution is slightly narrower for the case of EC-SeNPs, also indicated by the small degree of polydispersity (Table 1), meaning that *E. coli* was able to synthesize NPs with a more defined particle size.

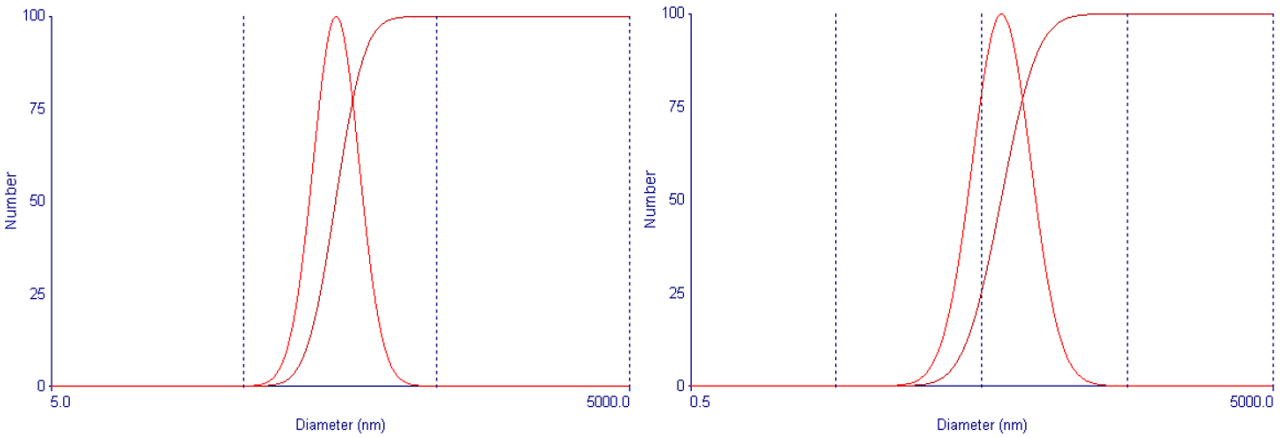

Figure 6. NP Size distribution of EC-Se (left) and SA-Se NPs (right) characterized by DLS.

For Z-potential and mobility measurements, a dip cell, containing two palladium electrodes, was submerged into the solutions. Then, an electric field was applied within the sample and the movement of the NPs from one electrode to the opposite under the effect of electrophoresis was characterized. The Z-potential indicates the surface charge of the NPs, which highly correlated to the type of biomolecules that compose the NP coating. All of them were negatively charged, possibly due to the presence of different functional groups coming from the bacteria. It can be noted that NPs synthesized by *E. coli* showed a lower surface charge compared to those synthesized by *S. aureus*, for which both CdSe and SeNPs showed very similar charge values. This is a clear evidence of the differences in composition of both coatings, as they come from different types of bacteria. The coating resulting from the synthesis with *S. aureus* had more negatively charged functional groups than that of *E. coli*. For the NPs coating coming from *E. coli*, the values varied noticeably between NPs. It could be that the different composition of those NPs could favor or disfavor the attachment of *E. coli*-derived functional groups. All in all, Z-potential remains an important parameter to study, not only because it gives an idea of the nature of the coating, but also because it provides a better understanding about the interaction between NPs and bacteria. S. Halder et al. reported the Z-potential for *E. coli* and *S. aureus*, to be -44.2 and -35.6 mV, respectively [70]. These values speak to the electrostatic behavior of the cells, which regulates the

bacterial adhesion [71] and contribute to the interaction with other agents [72]. This charge is due to the presence of several types of functional groups in bacterial membranes, such as acidic and basic functional groups, that are known to be associated with lipopolysaccharides (LPS), phospholipids (in the case of Gram-negative bacteria) or peptidoglycan and teichoic acid (in the case of Gram-positive bacteria) [73].

Table 1. Morphology, diameter, polydispersity, charge and mobility of the synthesized selenium based-NPs.

Type of NP	Morphology	Diameter (nm)	Polydispersity	Z-potential (mV)	Mobility (μm·cm/V·s)
EC-CdSeNPs	Spherical	175.6 ± 2.1	0.183	-16.86 ± 2.78	-1.29 ± 0.21
EC-SeNPs	Spherical	227.4 ± 1.3	0.097	-29.97 ± 1.54	-2.30 ± 0.12
SA-CdSeNPs	Spherical	166.9 ± 2.6	0.194	-40.68 ± 0.04	-3.01 ± 0.00
SA-SeNPs	Spherical	217.7 ± 1.6	0.254	-40.51 ± 0.11	-2.99 ± 0.01

Energy dispersive X-ray spectroscopy (EDX) measurements were performed in order to study the NP compositions (*Figure 7*). For the particular case of NPs made by *S. aureus*, EDX analysis showed the specific selenium absorption peak for SA-SeNPs and both selenium and cadmium peaks were present for SA-CdSeNPs. In the latter, there was a significantly higher amount of selenium compared to cadmium, which suggests that the cadmium reduction by bacteria is much less favorable than the selenium reduction. It could be because the cadmium reduction is thermodynamically less favorable, or because there is a lower number of enzymes able to reduce cadmium ions compared to those able to reduce selenium ions. Furthermore, there were peaks corresponding to carbon, oxygen and sulfur, which is most likely from the natural coating that comes from the bacteria. For SA-CdSeNPs, the intensity of the carbon peak was extremely high compared to SA-SeNPs, meaning that the coating-to-metallic core ratio was much more abundant for the SA-CdSeNPs. Moreover, in the case of SA-CdSeNPs, peaks corresponding to sodium and chloride were detected, which may come from the chemical washings applied in the purification

process that were not efficiently removed afterwards. Finally, the peak related to copper, present in both analysis, appeared due to the nature of the TEM grid used for the analysis.

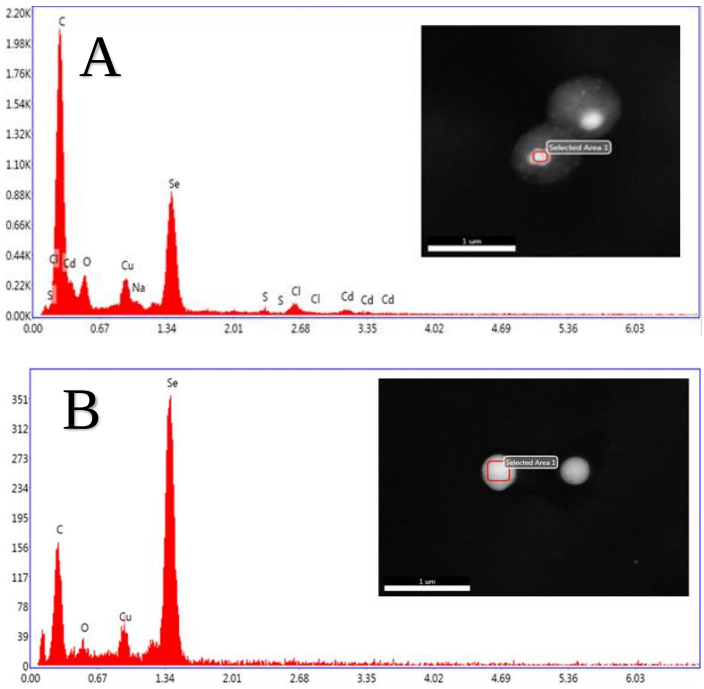

Element	Weight (%)	Atomic (%)
C K	59.71	83.18
O K	8.20	8.58
Cu L	5.63	1.48
Na K	1.08	0.78
Se L	19.85	4.21
S K	0.56	0.29
Cl K	2.27	1.07
Cd L	2.70	0.40

Element	Weight (%)	Atomic (%)
C K	43.00	78.14
O K	5.25	7.16
Cu L	5.78	1.99
Se L	45.97	12.71

Figure 7. EDX spectra, SEM image and composition table of SA-CdSeNPs (A) and SA-SeNPs (B).

3.1.3. Reaction kinetics

The kinetics of the reaction were studied in order to observe how the presence of different metallic salts interfere in the bacterial growth, compared to the growth in normal conditions.

In order to achieve this, bacterial growth was monitored by measuring the optical absorbance of *E. coli* and *S. aureus* at OD_{600} every 60 min from the beginning of the reaction for 8 h. The results showed that the bacterial growth in presence of Na_2SO_3 was very similar to the control, which indicates that bacteria were able to subsist despite the presence of selenium ions in solution. However, after 2 h, when the second metallic salt was added ($CdCl_2$ and $Zn(NO_3)_2{\bullet}(H_2O)_6$), both bacteria experienced a reduced growth rate compared to the control. This reduced rate is more pronounced in the case of the addition of $CdCl_2$ compared to $Zn(NO_3)_2{\bullet}(H_2O)_6$, which indicates

that cadmium ions present a higher toxicity than zinc ions. However, it should be noted that bacteria were still able to grow in spite of the presence of the metallic salts, meaning that they were able to cope with the salt toxicity by producing NPs. The tendencies observed and the reaction rates (*Tables 3* and *4*) were very similar for both types of bacteria. Nonetheless, *S. aureus* experienced a slightly higher growth in presence of $CdCl_2$ than *E. coli*.

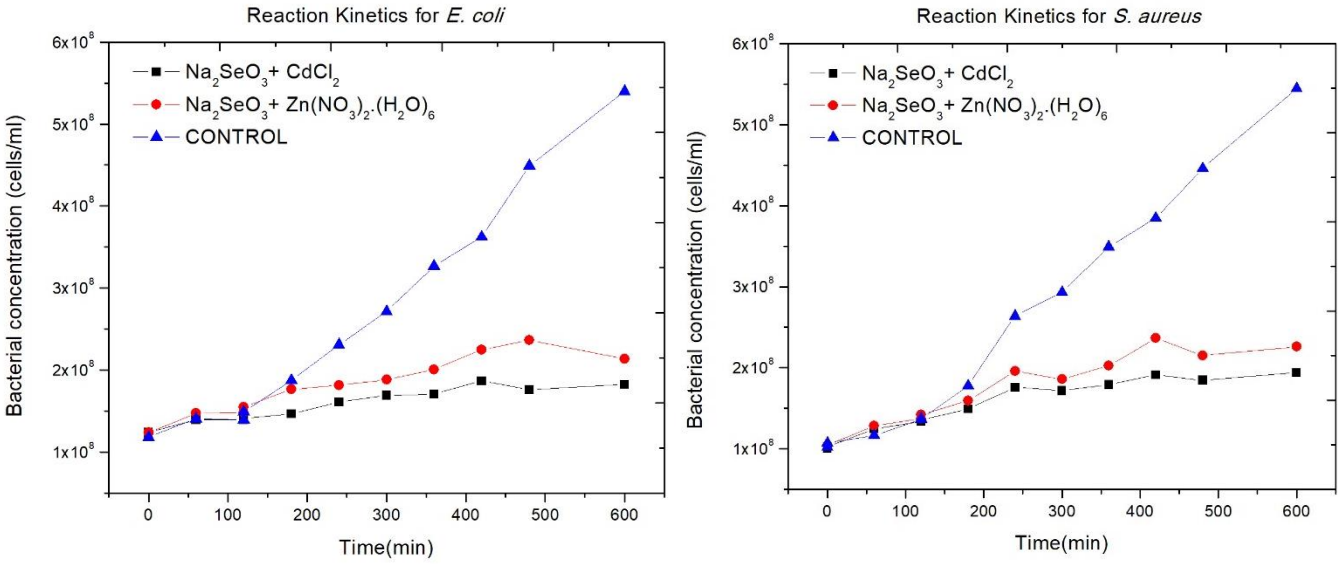

Figure 8. Absorbance monitoring for the reaction of synthesis of Se-NPs (red) and CdSe-NPs (black) by *E. coli* (left) and *S. aureus* (right) compared to a control (blue).

Table 3. Reaction rate and % respect to control for the synthesis made by *E. coli*.

Escherichia coli	**Reaction Rate (u.a./min)**	**% Respect to control**
Na_2SeO_3 + $CdCl_2$	4.72 E-05	17.09
Na_2SeO_3 + $Zn(NO_3)_2$	9.38 E-05	33.92
Control	2.76 E-04	100

Table 4. Reaction rate and % respect to control for the synthesis made by *S. aureus*.

Staphylococcus aureus	**Reaction Rate (u.a./min)**	**% Respect to control**
Na_2SeO_3 + $CdCl_2$	8.75 E-05	24.47
Na_2SeO_3 + $Zn(NO_3)_2$	1.15 E-04	32.23
Control	3.58 E-04	100

3.1.4. Effects of the initial concentration of the bacteria on the reaction

In order to study the effect of the initial concentration of bacteria on the reaction, the same synthetic route was followed, but with a starting concentration of 10^9 colony forming units (CFUs)/mL, which is ten times higher than was previously used.

During the reaction, a change of color to red was noticed after 1 h of the addition of Na_2SO_3, much earlier compared to 5 h corresponding to the previous accomplished synthesis with fewer bacteria. The color was much more intense than the one obtained by using a lower concentration of bacteria, which suggests a considerably higher production of NPs. However, the high concentration used impeded successful purification, as it was hard to separate all bacteria from the NPs. Thus, these NPs cannot be isolated efficiently if a more sophisticated purification process is not used. Nevertheless, the composition of the obtained powder after lyophilization was studied by X-Ray photoelectron spectroscopy (XPS). Peaks corresponding to the composition of bacteria and their biomolecules (such as carbon, sulfur, oxygen and phosphorus) were evident. Moreover, selenium and cadmium could be detected, strongly validating the ability of bacteria to reduce these ions.

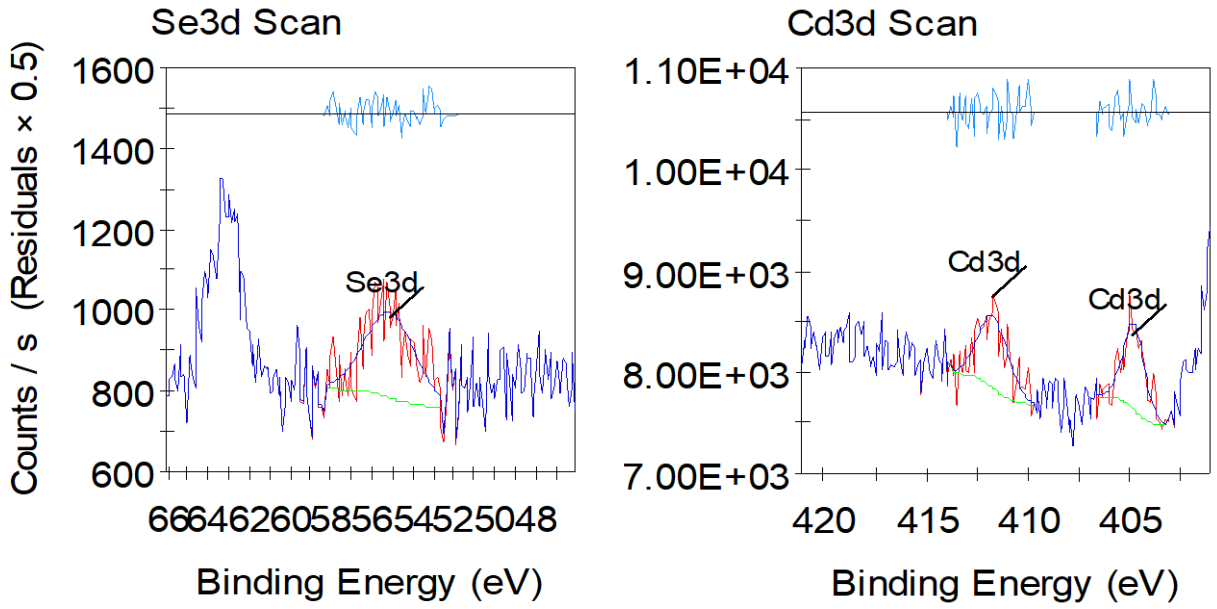

Figure 9. XPS spectrum of EC-CdSeNPs. Analysis obtained from the purified NPs deposited on carbon tape. Raw XPS data and peak fitting analysis represented together

3.1.5. Antimicrobial activity of selenium-based NPs

The antibacterial capability of the synthesized CdSe and SeNPs by *S. aureus* was tested by CFU assays, and the results are shown in *Figures 10* and *11*. Both bacteria, *E. coli* and *S. aureus*, were incubated for 8 h in presence of these NPs in order to study their proliferation upon exposure. As a general trend for all tested NPs, it can be inferred that, at low NP concentrations (5, 10 and 25 µg/mL), the bacterial concentration decreased with respect to the control, which was incubated in absence of NPs. However, at higher concentrations (50 and 75 µg/mL) the bacterial proliferation showed an increase in most of the cases, meaning a lower antibacterial efficiency. SA-SeNPs presented a higher antimicrobial activity compared to SA-CdSeNPs, as they decreased bacterial proliferation to a higher degree. For the case of SA-SeNPs tested against *S. aureus*, three concentrations of NPs (10, 25 and 50 µg/mL) showed a significant decrease of bacterial proliferation compared to the control, demonstrating the successful antimicrobial activity of SA-SeNPs.

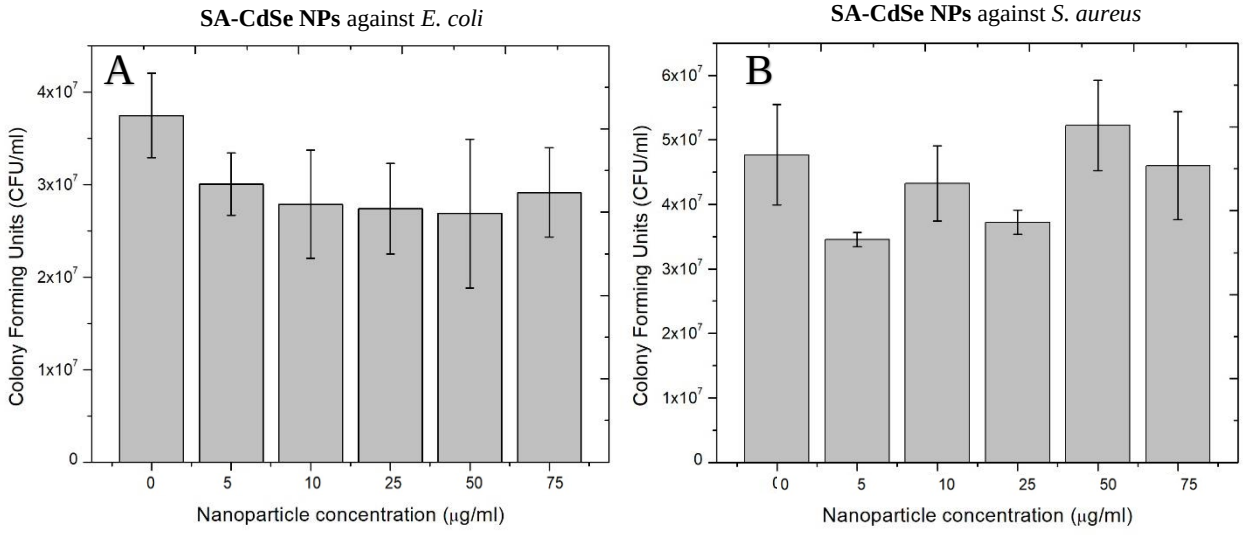

Figure 10. Colony Forming Unit assays for *E. coli* (A) and *S. aureus* (B) treated with SA-CdSeNPs during 8 h. Values represent the mean ± standard deviation of the mean. N=3.

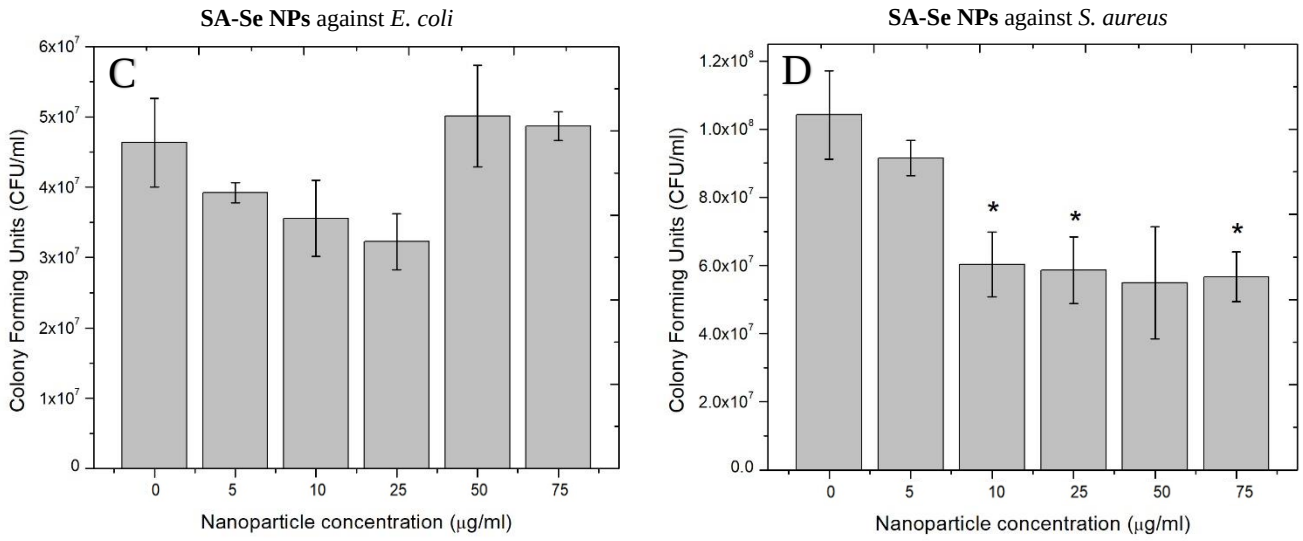

Figure 11. Colony Forming Unit assays for SA-SeNPs against *E. coli* (C) and *S. aureus* (D). Values represent the mean ± standard deviation of the mean. N=3. *p < 0.1 versus control.

The fact that higher concentrations of NPs tended to increase bacterial proliferation might be explained by the possible aggregation of NPs at high concentrations. When they aggregate, less NP surface is exposed to interact with external agents, resulting in a decrease in antibacterial efficiency [74].

Furthermore, SA-SeNPs, having a monometallic nature and higher diameter than SA-CdSeNPs, were more antimicrobial than their bimetallic counterparts. One hypothesis to explain this is the differences in the coating between the CdSe and SeNPs made by *S. aureus*. They were synthesized by the same bacterium, suggesting that the coating might be similar in composition, however, the NPs have an inherently different metallic-core, which could favor or disfavor the attachment of the specific protein components of the coating. This was verified by EDX analysis (*Figure 7*), in which the coating was much more prominent for the case of SA-CdSeNPs compared to SA-SeNPs, evidenced by the highly intense carbon peak present for the SA-CdSeNPs. Thus, depending on the thickness of the coating, which may in some cases fail to cover the entire NP surface, the bacterial activity may vary. In this case, it was observed that the NPs with a lower proportion of coating-to-core, SA-SeNPs, presented a higher antimicrobial effect. In addition, these NPs displayed a higher

antimicrobial activity against *S. aureus* compared to that against *E. coli*, probably because of the different natures of Gram-positive and Gram-negative bacteria, respectively. The main feature that distinguishes these two types of bacteria is the presence of an outer membrane formed by lipopolysaccharides and proteins in Gram-negative bacteria (*Figure 12*), specifically, which prevents agents from crossing the bacterial wall [75].

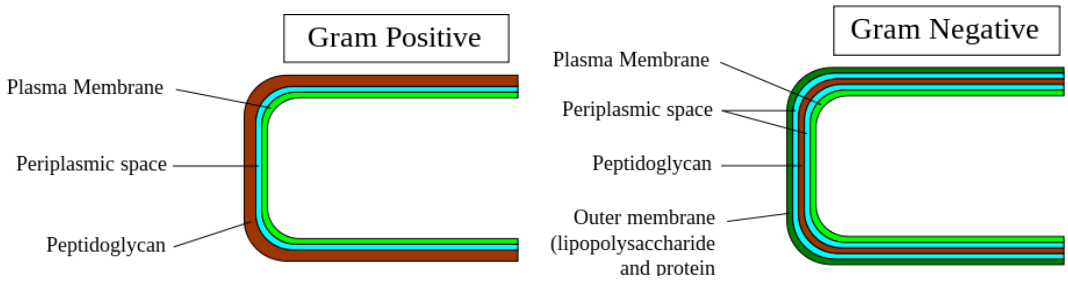

Figure 12. Differences in bacterial membrane for Gram-positive and Gram-negative bacteria. Image from *http://static.diffen.com/uploadz/0/0e/cell-wall-gram-bacteria.png*

By comparing the antimicrobial activity of SA-SeNPs with synthetic Se-NPs obtained by chemical methods from the literature [76], a similar trend against both bacteria could be observed. Synthetic Se-NPs at concentrations ranging from 10 to 50 affected significantly the growth of *S. aureus* whereas no effect was observed against *E. coli.* Nonetheless, the antimicrobial activity of SA-SeNPs against *S. aureus* was lower than the one obtained from synthetic Se-NPs; for the former, the antimicrobial activity was significantly reduced respect to the control with a p value of 0.1 at concentrations of 10, 25 and 75 µg/mL whereas for the latter the p value was 0.05. Otherwise stated, synthetic Se-NPs ensure antimicrobial activity with a 95% confidence level compared to a 90% for SA-SeNPs. It should be noted that the treatment time for synthetic Se-NPs was 15 h instead of 8 h for this study. Moreover, these synthetic Se-NPs presented a lower size (79 nm), which can definitely influence the activity against bacteria.

The antimicrobial activity of these NPs can be explained in terms of two main mechanisms: (1) the production of reactive oxygen species (ROS), and (2) the release of metal ions from the nanostructures. The former, ROS species, are chemically reactive agents containing oxygen within the molecules, such as hydroxyl (OH^-) or superoxide (O_2^{2-}) groups. These species normally result from the metabolism of oxygen in cells; however, ROS exposure at higher concentrations than normal physiological levels can lead to serious cell damage. Metallic NPs are involved in the increase of ROS production, leading to the interruption of several metabolic routes essential for cell viability. The second main mechanism through which NPs can alter bacterial growth is the release of metal ions from the nanostructures. Metal ions are typically absorbed by the cell membrane and can therefore directly interact with its components. This interaction leads to extensive inhibition of enzymatic activity, not only changing the cell structure but also affecting the rates of physiological processes such as cell respiration, which causes general dysfunction within the bacteria. Therefore, it is believed that the presence of metallic NPs induces the formation of ROS together with the release of metal ions, leading to a systemic failure of the internal metabolism.

3.1.6. Detection of reactive oxygen species (ROS)

As stated in the "Antibacterial assays" section, one of the main mechanisms of the antimicrobial activity of NPs is the production of ROS, able to induce bacterial cell membrane damage, proteins, DNA and intracellular systems such as the respiratory system [77]. In this study, the production of ROS was detected by using DCFDA. After 8 h of incubation, as it can be seen in *Figure 13*, Se-NPs recorded the highest fluorescence intensity, which is proportional to the concentration of ROS. This indicates a higher ROS production from Se-NPs compared to both CdSe-NPs and the control, and supports the results from the colony counting assays. However, this increase was not

significant with respect to the control, which suggests that there are probably other mechanisms taking part in the antimicrobial activity of these NPs, such as the release of metal ions.

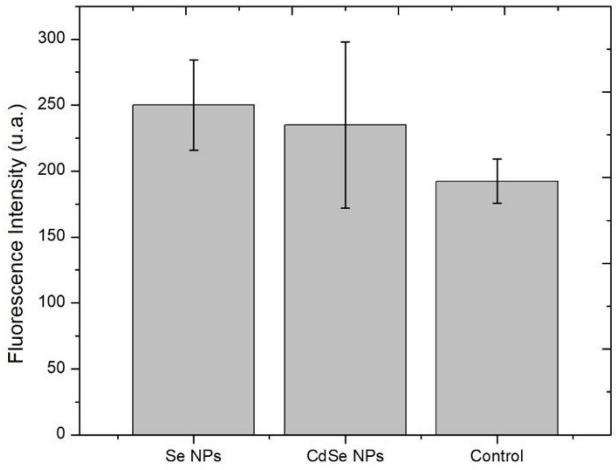

Figure 13. Formation of ROS in *E. coli* cells treated during 8 hours with 100 µg/ml SA-SeNPs and SA-CdSe NPs. Values represent the mean ± standard deviation of the mean. N=3. The control was not treated.

3.1.7. In vitro cytotoxicity assay

Human dermal fibroblasts (HDF, passage number 4) cells were used to perform in vitro cytotoxicity assays to test the biocompatibility of Se and CdSe NPs. The effects of the NPs at concentrations ranging from 5 to 75 µg/mL in HDF cells were studied over several periods of time: 1, 3 and 5 days (*Figure 14*). The passage number of the cell culture used was 4.

From the results, all the tested concentrations ranging from 5 to 75 µg/mL presented a high level of cell viability during the periods of time studied (1,3 and 5 days). Interestingly, the cell proliferation was not negatively affected by the presence of these two types of NPs, but it was actually improved. This unexpected tendency is especially pronounced for the case of HDF cells treated with NPs for 1 day. Research studies have shown an increase in DNA content in cells exposed to NPs. Sun Q. et al. observed that the exposure to TiO_2-PEG NPs at doses lower to 100

μg/mL led to cell proliferation [78]. They also noticed the aggregation of growth factor receptors on the surface of cells exposed to those NPs, what increased the cell growth rate.

Another possible explanation for this tendency could be that the natural coating surrounding the NPs provides nutrients for these cells, as it is composed of biomolecules such as lipids and proteins that originally came from the bacteria. Therefore, these nutrients could also improve fibroblast proliferation.

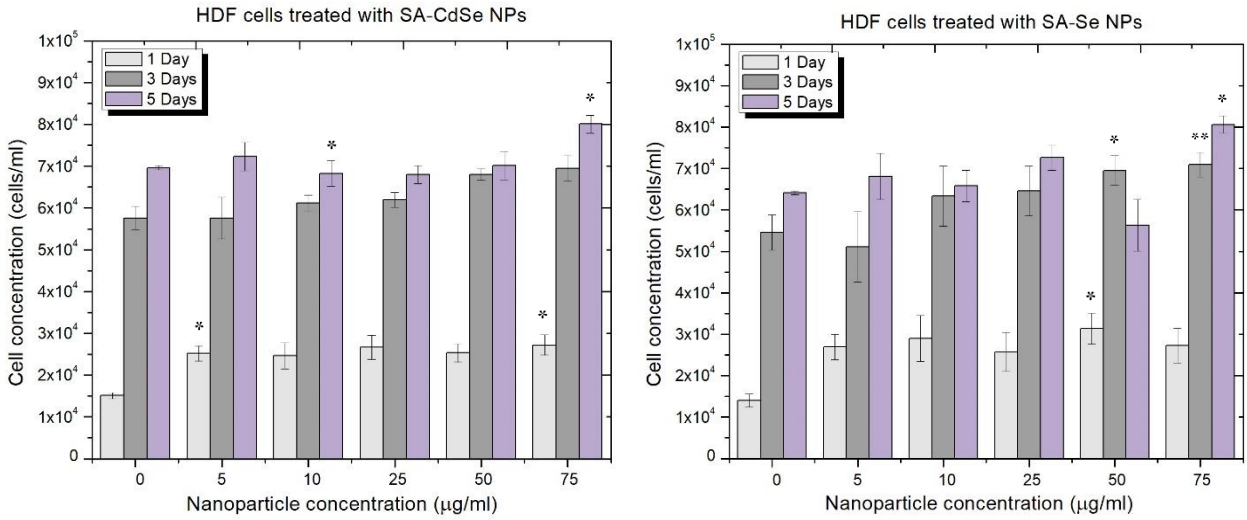

Figure 14. ***In vitro*** **cytotoxicity of HDF cells treated with CdSe and Se NPs for 1, 3 and 5 days.** The study was assessed by MTS assays. Values represent the mean and standard deviation, N=3. *p<0.05, **p<0.01 versus the control at the same period.

The literature shows that, for synthetic Se-NPs, there is a reduction in cell viability up to a maximum of 30% for concentrations ranging from 10 to 50 μg/mL [76]. This result clearly showed the significant enhancement in biocompatibility for biogenically synthesized Se-NPs compared to synthetic Se-NPs, thus being highly suitable for biomedical applications.

3.2. <u>Objective II</u>: Synthesis of Se-NPs by *H. pylori* to develop a novel route to treat its infection.

3.2.1. Synthesis

With the objective of exploring the synthesis capabilities of *Helicobacter pylori* (*H. pylori*) for the production of NPs, the bacterium was inoculated with a selenium metallic salt, subsequently producing Se-NPs. This demonstrated, for the first time to our knowledge, the ability of this type of bacterium to reduce metal ions into NP.

The synthesis was achieved by adding different concentrations of Na_2SeO_3 (1, 2 and 5 mM) into a bacterial culture previously adjusted to a concentration of 10^8 cells/mL. After the addition, the culture was left for 72 h and the obtained NPs were purified. The solution turned red after 5 h of inoculation, which is representative of the reduction of SeO_3^{2-} to Se^0. *Figure 15* shows the different colors of the cultures after 24, 48 and 72 h of inoculation. The solution that acquired the more intense color corresponds to the one to which the highest concentration of metal was added (5 mM Na_2SeO_3) indicating a larger NP diameter and/or higher yield of NPs with respect to the others.

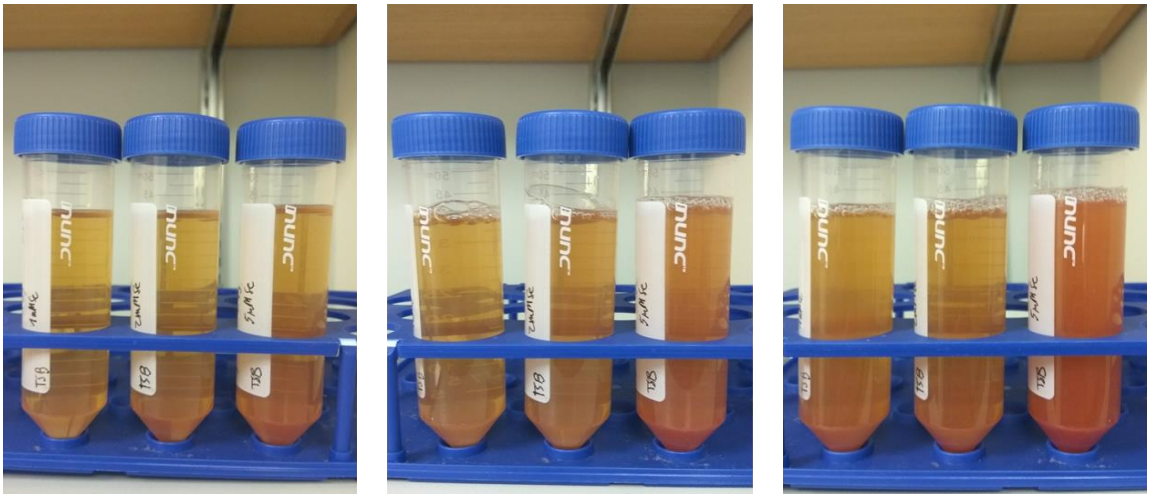

Figure 15. Color change during the reaction after 24 h (A), 48 h (B) and 72 h (C). The falcon tubes correspond, from left to right, to the reaction adding 1 mM, 2 Mm and 5 mM *Na_2SeO_3*.

To demonstrate that bacteria are responsible of the reduction of the selenium salt, the same reaction was tested in TSB medium without adding bacteria. No color change was noticed, indicating that the TSB components were not able to reduce the selenium oxyanion.

After purification and resuspension of the synthesized Se-NPs into distilled water, the solutions presented the color shown in *Figure 16*.

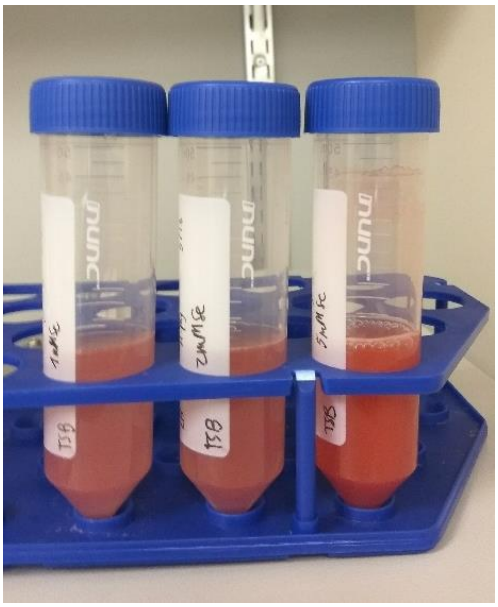

Figure 16. Color of the NPs resuspended in water. The falcon tubes correspond, from left to right, to the reaction adding 1 mM, 2 Mm and 5 mM.

3.2.2. Characterization

The morphology of the Se-NPs obtained by the synthesis route using 5 mM Na_2SeO_3 was investigated by TEM (*Figure 17*). The bacterium was able to produce relatively homogeneous NPs with a round shape. Most of the NPs presented sizes from 120 nm to 170 nm, however, there were also particles, at a much lower frequency, with diameters of nearly 500 nm.

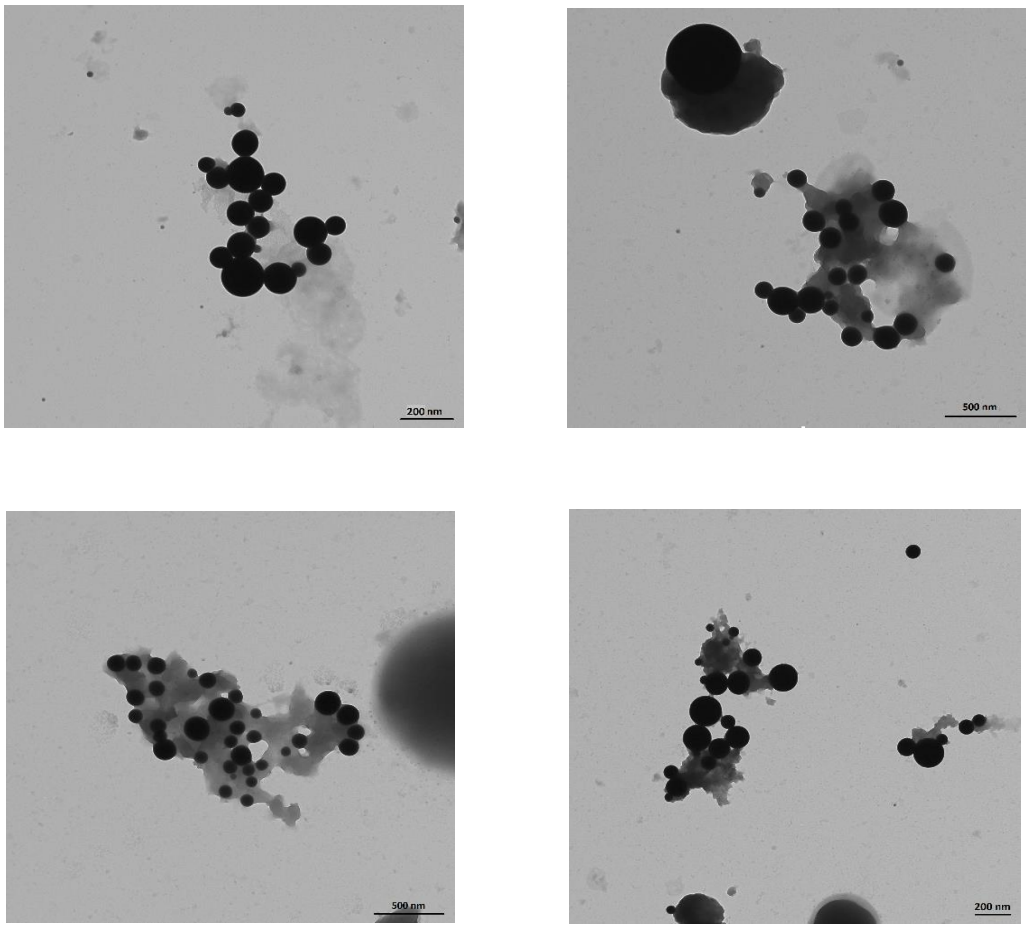

Figure 17. TEM images of Se-NPs made by *H. pylori* via the addition of 5 *mM* Na_2SeO_3.

The diameter and polydispersity of the NPs obtained by adding different concentrations of Na_2SeO_3 (1, 2 and 5 mM) were investigated by DLS. The following nomenclature was used to denote them: 1-SeNPs, 2-SeNPs and 5-SeNPs, respectively. The values obtained are shown in *Table 4*.

Different sizes and values of polydispersity were obtained for each type of NP. The lowest diameter obtained was for 2-SeNPs, although the polydispersity is high, meaning that the NP size distribution covers a wide range of values. The lowest polydispersity, which denotes a narrow NP size distribution, was obtained for 1-SeNPs. This shows that the lower range of NP sizes was obtained when adding the lowest concentration of salt.

Table 4. Morphologic characterization and Z-potential studies of different Se-NPs.

Type of NP	Nomenclature	Morphology	Diameter (nm)	Polydispersity	Z-potential (mV)	Mobility (µm·cm/V·s)
SeNPs (1mM salt)	1-SeNPs	Spherical	168.6 ± 1.0	0.099	-22.27 ± 0.84	-1.71 ± 0.06
SeNPs (2mM salt)	2-SeNPs	Spherical	142.8 ± 1.4	0.279	-37.45 ± 1.48	-2.87 ± 0.11
SeNPs (5mM salt)	5-SeNPs	Spherical	190.1 ± 1.9	0.208	-40.58 ± 0.06	-3.00 ± 0.00

The Z-potential and NP mobility were explored by using the same instrument, DLS, but in this study, a dip cell containing two electrodes needs to be introduced into the solution in order to characterize the charge and mobility of the NPs. As it can be seen in *Table 4*, the surface charge varied between the different NPs, meaning that the concentration of selenium salt influences the final surface charge of the formed NP. The higher metallic salt concentration, the more negatively charged the NPs produced were. Bhattacharjee S. from the University College of Dublin, indicated that Z-potential values higher than ± 30 mV meant a stable suspension [79]. This means that 5-SeNPs are preferred, as they exhibit a better stability in solution.

The composition of 5-SeNPs was proved by XPS analysis (*Figure 18*), clearly showing a peak corresponding to the presence of selenium.

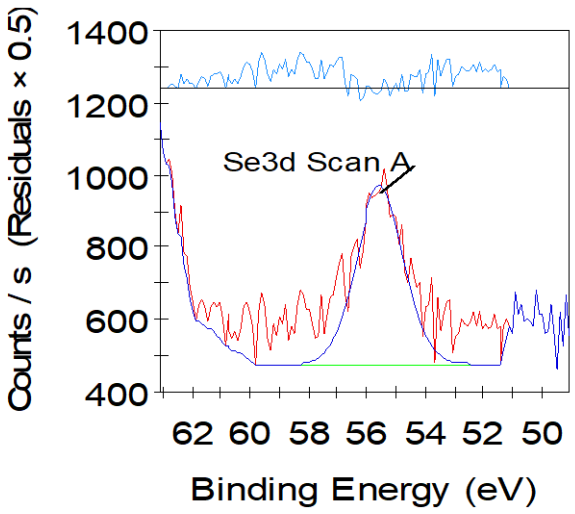

Figure 18. XPS spectrum of 5-SeNPs. Analysis obtained from the purified NPs deposited on carbon tape. Raw XPS data and peak fitting analysis represented together.

3.2.3. Effect of different selenium salts on bacterial growth

The aim of this study was to elucidate how *H. pylori* responds to the addition of different selenium salts at different concentrations. To achieve this, *H. pylori* was cultivated for 24 h in presence of these salts and its growth analyzed by measuring optical absorbance of the culture every 2 min. The following salts were studied: sodium selenite (Na_2SeO_3), sodium selenate (Na_2SeO_4), selenous acid (H_2SeO_3) and sodium biselenite ($HNaO_3Se$), at different concentrations (5, 4, 3, 2, 1, 0.5 and 0.1 mM).

First, the ability of *H. pylori* to reduce the different salts into elemental selenium was noted by observing the color of the solutions. A color change to red indicates the reduction of selenium ions into elemental selenium, most probably in the form of NPs. In contrast, no change of color, thus remaining similar to the control of just the salt and media, shows that the bacterium were not able to reduce the selenium salt. The resulting solutions, shown in *Figure 19*, present a color change after 24 h of incubation for the case of Na_2SeO_3, H_2SeO_3 and $HNaO_3Se$, indicating that the enzymes present in *H. pylori* were capable of reducing the ion SeO_3^{2-} into elemental selenium, independent of the molecular source of the ion (different selenium salts). Specifically, in the case of H_2SeO_3, no color developed at higher concentrations, which remained a clear yellowish color. The acidic nature of this salt induced a higher toxicity to bacteria compared to the rest. However, at low concentrations (1, 0.5 and 0.1 mM), bacteria could survive the acidic environment, and were able to produce selenium from the oxyanion. For the case of Na_2SeO_3 and $HNaO_3Se$, the red color appeared even at high concentrations, thereby indicating the lower toxicity of these salts. However, it should also be noted that there were a slightly higher number of wells with red-colored solutions for the case of Na_2SeO_3 compared to those of $HNaO_3Se$.

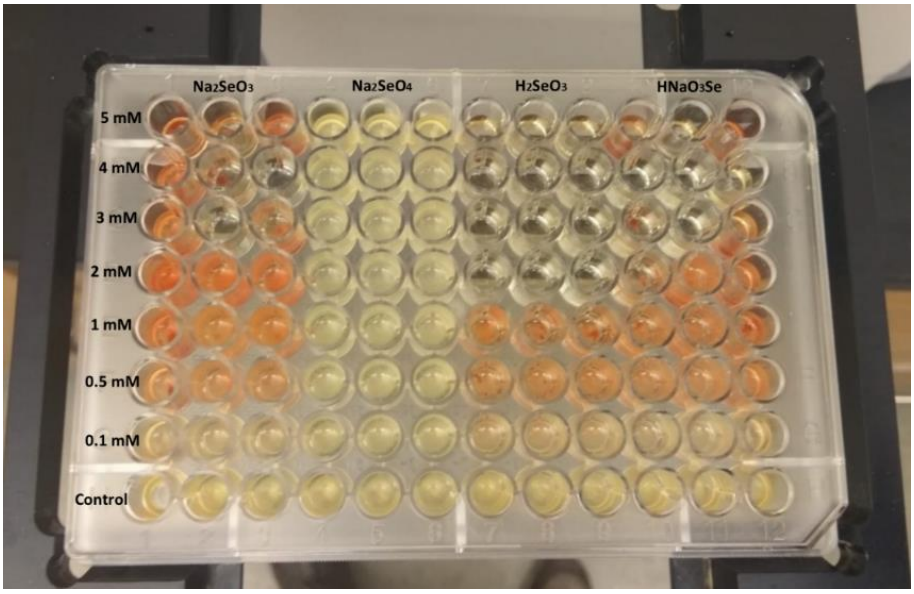

Figure 19. Color change in bacterial solutions incubated with different selenium salts at different concentrations for 24 hours.

Unlike the other three salts, bacteria incubated with Na_2SeO_4 did not develop red color at any concentration, meaning that there was a lack of enzymes present in *H. pylori* able to reduce the selenate anion, SeO_4^{2-}. Moreover, the solutions presented a cloudy yellow color, meaning that the bacteria were still able to grow in spite of the presence of Na_2SeO_4.

In order to study the bacterial growth in a quantitative manner, the absorbance of the bacteria at 600 nm was measured every 2 min for 24 h after the addition of the metallic salts. This study enabled us to choose both the optimal compound and concentration for the production of NPs. It should allow bacteria to grow, although it would not be in their optimal environment, in order to ensure a good NP yield. The bacterial growth curves corresponding to different selenium salts are plotted in *Figures 20* and *21*.

For the case of Na_2SeO_3 and $HNaO_3Se$, the concentrations of metallic salt higher than 1 mM first inhibited the growth; however, after 7 h of incubation, bacteria were able to successfully elude the toxicity of the salt, experiencing a jump in their growth. In contrast, the lowest concentrations,

specifically 0.1 and 0.5 mM, slightly slowed down the growth but did not show any significant repercussion.

The addition of H_2SeO_3 resulted in a complete growth inhibition at concentrations higher than 1 mM. Nevertheless, at lower concentrations, bacteria became tolerant and started to grow, although they did not suffer a pronounced increase as in the case of Na_2SeO_3 and $HNaO_3Se$.

As previously stated, for Na_2SeO_4, no NPs were formed, meaning that *H. pylori* is not able to reduce selenate anions. It can also be stated that the salt was not highly toxic to bacteria, as at all tested concentrations, the growth was barely affected and was similar to the control in which bacteria grew at normal conditions (without selenium salt).

All in all, the metallic salt that allowed the best bacterial growth was Na_2SeO_3, followed by $HNaO_3Se$. The curves corresponding to 2 and 1 mM for both salts experienced an enormous jump in growth, meaning that they were suitable concentrations for the production of NPs, as the growth rate improved during the first 24 hours of incubation.

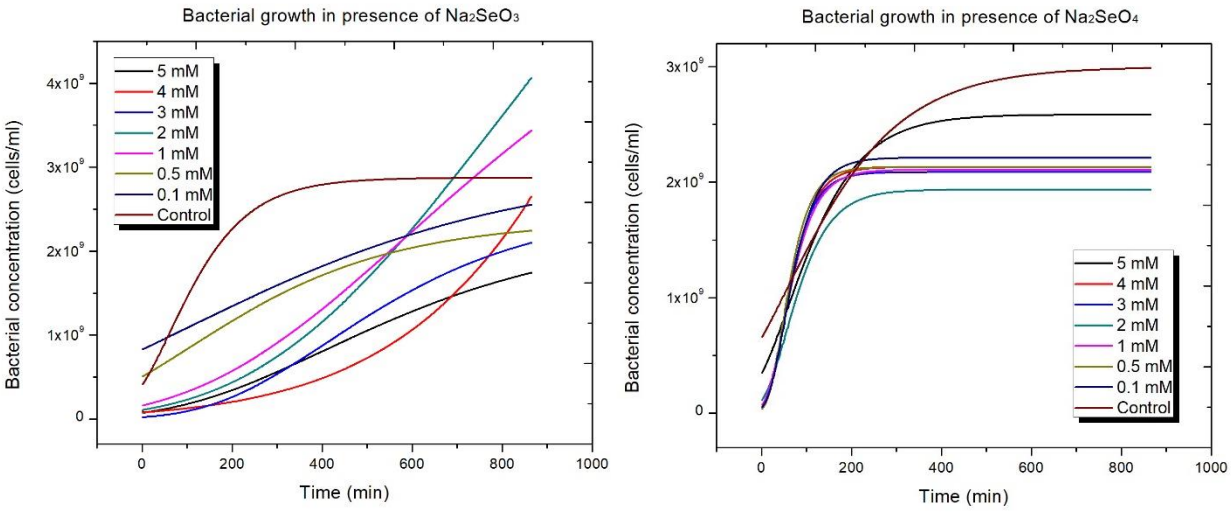

Figure 20. Bacterial curves for *H. pylori* incubated with different concentrations of Na_2SeO_3 and Na_2SeO_4 for 24 hours. Graphs were fitted using Gompertz modelization.

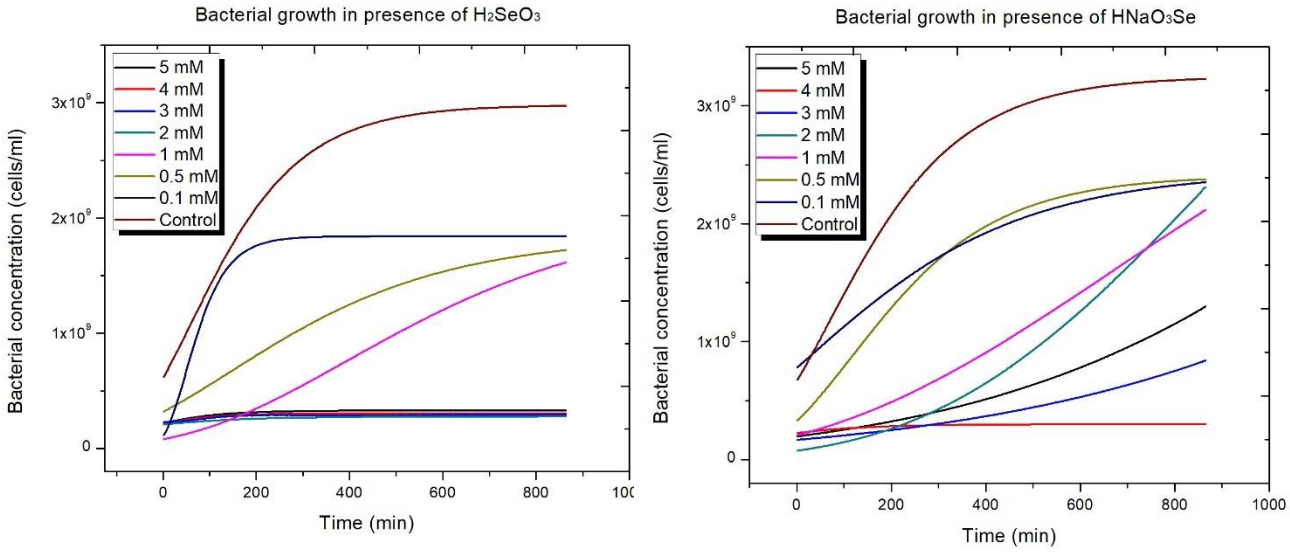

Figure 21. Bacterial curves for *H. pylori* incubated with different concentrations H_2SeO_3 and $HNaO_3Se$ for 24 hours. Graphs were fitted using Gompertz modelization.

3.2.4. Antimicrobial activity by growth curve analysis

The antimicrobial capabilities of the synthesized 1-SeNPs, 2-SeNPs and 5-SeNPs were tested by growth curve assays. *H. pylori* was incubated in the presence of different concentrations of these NPs for 24 h, and its growth monitored by absorbance. According to the results shown in *Figure 22*, it can be clearly seen that the NPs that produced the least antimicrobial effect were 1-SeNPs, as most of the curves obtained were similar to the control. Unexpectedly, the concentration that presented the highest effect against bacteria was 25 μg/mL, suggesting that the optimal concentration of NPs is in the mid-range (for the range between 5 and 100 μg/mL).

Comparing 2-SeNPs and 5-SeNPs, the bacterial growth was more influenced by the presence of the latter. In the case of 5-SeNPs, there was a clear distinction between the higher concentrations (100, 75, 50 and 25 μg/mL), which strongly affected the growth, and the lowest ones (10 and 5 μg/mL), that barely showed any difference with the control.

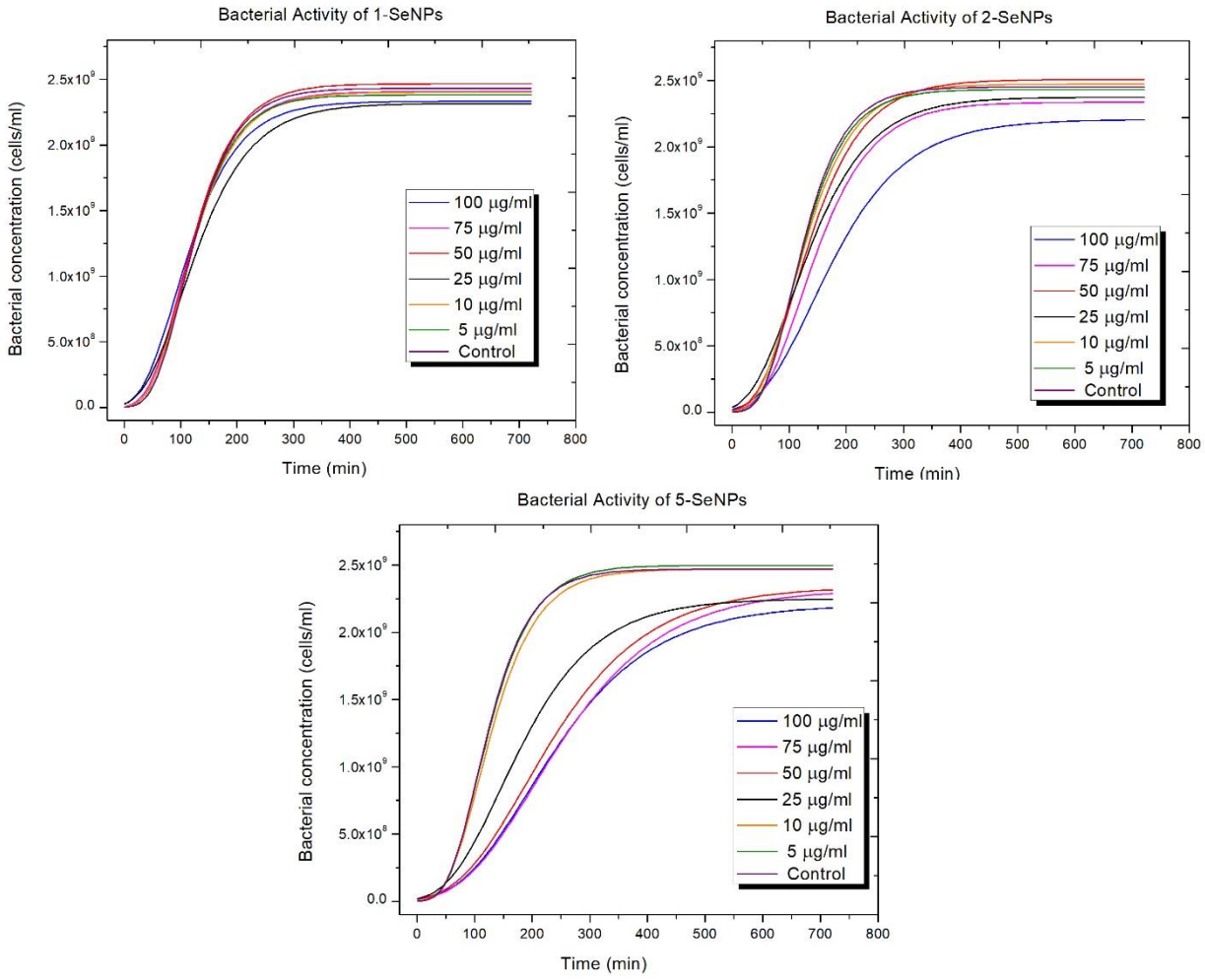

Figure 22. Bacterial growth assay for *H. pylori* incubated with different concentrations of 1-SeNPs, 2-SeNPs and 5-SeNPs for 24 hours. Graphs were fitted using Gompertz modelization.

In order to further study the significance of these curves, the modified Gompertz model was applied. The original Gompertz equation describes a sigmoidal growth curve, containing mathematical parameters (*a*, *b*, *c*) rather than biological ones, as show in *Equation 1*.

$$y = a \cdot e^{-be^{-ct}} \qquad \text{(Eq. 1)}$$

It is not possible to estimate the biological parameters nor the errors accurately from this mathematical equation. Instead, it was rewritten in order to directly express the biological parameters, *A*, μ and λ, as shown in *Equation 2*.

$$y = A \cdot e^{-e^{\left(\frac{\mu \cdot e}{A}\right)\cdot(\lambda - t)+1}} \qquad \text{(Eq. 2)}$$

This expression, known as the modified Gompertz equation, was obtained through a series of derivations and was the one used for fitting bacterial growth curves. In contrast to the original equation, the parameters of this equation have biological meaning rather than mathematical.

The parameter *y* corresponds to the optical density reading, directly proportional to the concentration of bacteria, *A* is the asymptote, μ is the maximum exponential growth rate and λ is the lag time. These parameters were estimated according to a least-squares estimation algorithm using a GRG nonlinear solver. All of them were calculated and plotted for analysis. The data was collected for *H. pylori* in presence of the three types of NPs and results are shown in *Figure 23.*

The parameter *A* represents the maximum specific growth of the bacteria under experimental conditions. While analyzing the results, it was found that NP concentrations of 25 and 100 μg/mL led to a lower asymptotic absorbance value. This was observed especially for the case of 2-SeNPs at 25 μg/mL and 5-SeNPs at 100 μg/mL, meaning that these NPs at these concentrations present high antimicrobial activity.

The maximum exponential growth rate was studied by analyzing the parameter μ. As a general trend, the graph showed that higher NP concentrations resulted in a lower growth rate. This tendency can be clearly detected for 5-SeNPs, however, for the case of 1-SeNPs and 2-SeNPs, the concentrations that presented a higher impact in decreasing the rate were 25 and 100 μg/mL.

The parameter λ represents the lag time in the bacterial growth under experimental conditions. For the case of 5-SeNPs, the lag time increased as the nanoparticle concentration increased. This tendency could be observed for 2-SeNPs at higher concentrations than 25 μg/mL. In contrast, for the case of 1-SeNPs, a clear tendency in the lag time could not be observed.

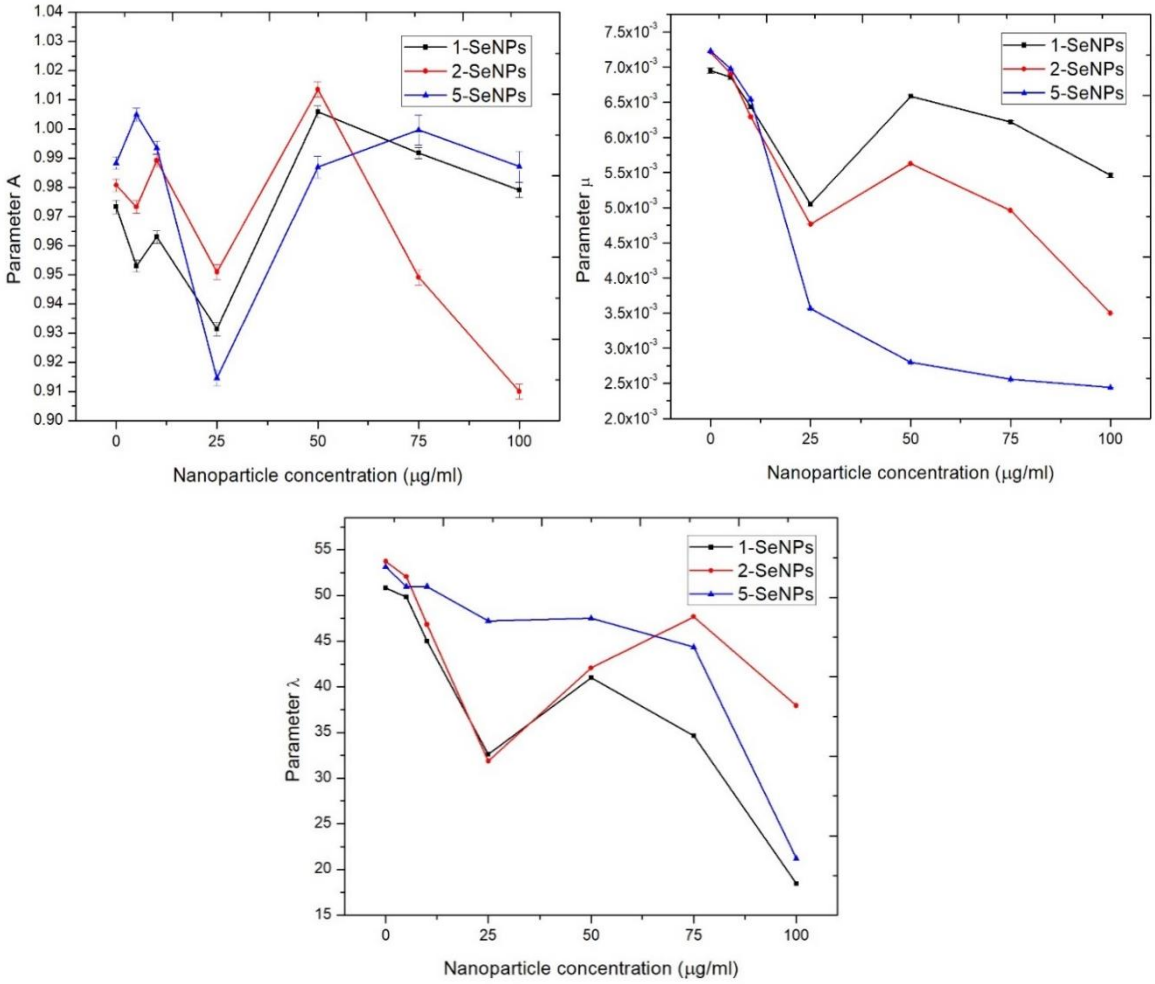

Figure 23. Analysis of parameters *A*, *μ* and *λ* from the modified Gompertz equation from the bacterial curves shown in *Figure 22*.

It is expected that the presence of NPs might cause a delay in the maturing of bacteria, as they need to adapt themselves to the new growth conditions, different from the ones they are used to live. Therefore, this environment is preventing them to accomplish cell division in the way they should, affecting their growth cycle.

This delay can be clearly observed for the case of 5-SeNPs, which have already been demonstrated to present the highest ability to stop bacterial growth. Then, 2-SeNPs showed an increased delay in bacterial growth at higher concentrations than 25 μg/mL. Lastly, as it was expected, 1-SeNPs did not produce any delay in the growth, what matches with the low antimicrobial activity observed in previous results.

Therefore, as a conclusion for the analysis of Gompertz parameters, 5-SeNPs presented the highest impact in bacterial growth, as they decreased bacterial absorbance at a high level, decreased the maximum growth rate and finally, caused a delay in the lag phase.

3.2.5. Colony forming units assay

The antimicrobial activity was studied for 5-SeNPs, as these NPs provided the highest action against bacteria in the previous study. To accomplish this, *H. pylori* was incubated for 8 h in presence of different concentrations of 5-SeNPs (5, 10, 25, 50 and 75 µg/mL). These treated bacteria were later inoculated into agar plates to study their ability to give rise to colonies. The number of colonies generated were counted and the data was treated, and the results are shown in *Figure 24*.

From the figure, it is clear that there is a homogeneous decreasing trend of the bacterial proliferation upon an increase in NP concentration. For 10 µg/mL, there was a significant difference of CFUs with respect to the control, indicating that 5-SeNPs at this mentioned concentration showed clear antimicrobial activity.

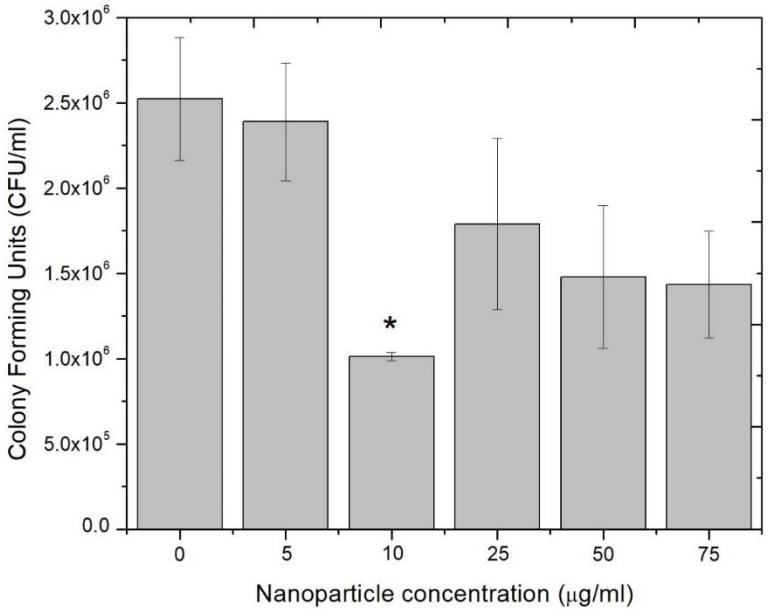

Figure 24. Colony counting of *H. pylori* treated with different concentrations of 5-SeNPs.
Values represent the mean ± standard deviation of the mean. N=3. *p < 0.1 versus control.

It is noteworthy to mention that results from the growth curve assays and the colony counting unit assays might not always coincide, as bacteria are exposed to different growth conditions in each type of assay; liquid media for growth curve assay and solid media for colony counting assay. Previous reports show that stress-injured cells perform better in liquid media rather than solid media [80]. Also, bacteria could be stressed due to the transfer from liquid medium to solid medium when preparing the plates for colony counting [81].

3.2.6. In vitro cytotoxicity assay

The cytotoxicity of 5-SeNPs was studied in HDF cells during 1, 3 and 5 days (*Figure 25*). The passage number of the cell culture used was 5. Of all the tested concentrations ranging from 5 to 75 μg/mL, the only one that did not present cytotoxic effects against HDF during all the time periods tested was 5 μg/mL. At concentrations of 10 μg/mL, the effect of 5-SeNPs was barely noticeable after 1 day of incubation; however, there were significant differences after 3 and 5 days, showing clear cytotoxicity.

Thus, 5-SeNPs can only be considered biocompatible for concentrations lower than 5 μg/mL. In the case of 10 μg/mL, they do not affect healthy cells if they do not exceed 24 hours of contact with them. Common drugs orally ingested to treat *H. pylori*, such as a combination of amoxicillin, lansoprazole and clarithromycin, remain in the body up to 8 hours, being excreted in the urine. This exemplifies a treatment that requires much less than 24 hours to accomplish its action. Furthermore, according to the previous colony counting studies, the time needed for 5-SeNPs to significantly affect bacterial growth was 8 h, time period in which no cytotoxic effects were observed.

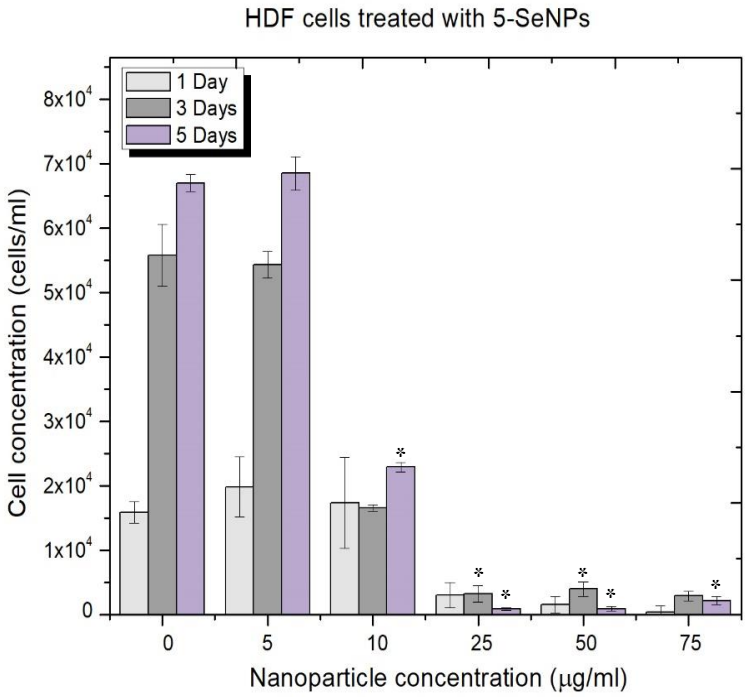

Figure 25. *In vitro* cytotoxicity of HDF cells treated with 5-SeNPs for 1, 3 and 5 days. The study was assessed by MTS assays. Values represent the mean6standard deviation, N=3. *p<0.01 versus the control at the same time period.

By comparing these results with synthetic Se-NPs from the literature, a higher cytotoxicity was obtained for 5-SeNPs synthesized by *H. pylori* compared to synthetic Se-NPs obtained via a chemical method [76]. This increased cytotoxicity might be due to the coating composed by biomolecules (proteins and lipids) from *H. pylori*, which might be pathogenic to human healthy cells.

As the coating resulted to negatively affect cell proliferation, alternatives should be taken to elude these cytotoxic effects; such as the design of a purification process (via ultrasonication, harsh chemical washes, …) that removes a sufficient part of this coating that avoids its cytotoxic effect.

4. CONCLUSIONS AND FUTURE PROSPECTIVES

Over the years, many microorganisms exposed to antibiotics have adapted to these compounds. The broad and vast use of antibiotics for medical, veterinary, and agricultural purposes has led to an increasing emergence of antibiotic-resistant strains of pathogenic bacteria. As a result, antimicrobial resistance (AMR) is now one of the most serious problems worldwide.

The emergence of resistant strains has made it imperative to search for novel methods that abstain from the use of antibiotics. Therefore, the application of nanotechnology in pharmaceuticals and microbiology has gained prevalence to prevent the catastrophic consequences of AMR. Among all nanomaterials, metal NPs are potential candidates to deal with emergent resistant strains. They have shown an enormous capacity in different studies to effectively cope with a broad spectrum of antibiotic resistance bacteria [82].

Common routes to synthesize metal NPs are based on physico-chemical routes; however, these procedures have disadvantages such as extreme reaction conditions, production of toxic byproducts, and the requirement of addition steps for functionalization, among others. Thus, biogenic synthetic routes have been proposed as alternatives to overcome these drawbacks. Specifically, the use of bacteria to synthesize nanomaterials is a green and cost-effective route to produce NPs in an eco-friendly way and without the need of additional functionalization steps. Therefore, the aim of this project was to explore the synthesis capabilities of bacteria to produce selenium-based NPs and study their potential for biomedical applications. (cells/cm^2)

4.1. <u>Objective I</u>: Synthesis of selenium based metallic NPs by *E. coli* and *S. aureus.*

In the first objective of the project, the synthesis of CdSe and SeNPs by *E. coli* and *S. aureus* was achieved. Both bacteria were able to successfully reduce selenium and cadmium metallic salts (Na_2SeO_3 and $CdCl_2$) into NPs, but were unsuccessful for zinc salt ($Zn(NO_3)_2•(H_2O)_6$) due to a possible lack of enzymes for the reduction of the zinc ion specifically. The characterization showed equal morphologies and similar sizes for all the synthesized NPs; however, the surface charge and mobility given by Z-potential studies correlated with the type of bacteria used for synthesis. This strongly suggests that the coating of the NPs possessed bacteria-specific compositions, meaning that the functional groups varied depending on the bacteria that synthesized the NPs. EDX characterization afforded the determination of the bi- and monometallic nature of CdSe and SeNPs, respectively, together with the specific composition of the bio-coatings consisting of carbon, oxygen and sulfur. These coatings were much abundant in the case of the BNPs, suggesting that the coating chemically favored the BNPs and remained more strongly attached.

From the study of the kinetics of the reaction, the presence of the different metallic salts affected the growth. However, it was not completely inhibited, and allowed bacteria to deal with the toxicity of the salts by producing NPs.

The CFU assays to test the antimicrobial activity of the NPs synthesized by *S. aureus* against both Gram-negative and Gram-positive bacteria showed that major bacterial growth inhibition was accomplished by SA-SeNPs against *S. aureus*. It was hypothesized that the lower proportion of coating-to-metallic core for SA-SeNPs compared to SA-CdSeNPs led to an increased antibacterial activity. Moreover, the fact that these monometallic NPs exhibited a higher effect against *S. aureus* than against *E. coli* can be explained by the different nature of both bacteria. Gram-positive bacteria, such as *S. aureus*, remain more susceptible to the attack of external agents, as they possess only one cell membrane in contrast to the double membrane of Gram-negative bacteria such as *E.*

coli. Therefore, the latter are able to prevent certain drugs and antibiotics from penetrating the cell, and are thus more resistant to the action of drugs.

The *in vitro* cytotoxicity assays of SA-CdSe and SA-SeNPs revealed no significant cytotoxic effects to HDF cells during 1, 3 and 5 days of incubation. Surprisingly, the presence of the NPs produced an *improvement* of the cell viability, especially for the 1-day incubation. This enhancement could be due to the possible aggregation of NPs, which might involve a starting point for cell growth. Moreover, the biological nature of the coating surrounding the NPs might serve as nutrients for the human cells, increasing their proliferation.

Hence, the ability of E. coli and S. aureus to produce bi- and monometallic selenium-based NPs (CdSe and Se) has been demonstrated. The antimicrobial assays demonstrated that SA-SeNPs presented high antimicrobial activity, notably more significant against Gram-positive bacteria compared to Gram-negative. These results are in agreement with previous studies with synthetic Se-NPs [76], although the activity of biogenic selenium based NPs has resulted to be less than the achieved with synthetic Se-NPs. Moreover, the biocompatibility of the NPs synthesized by *S. aureus* was validated for HDF cells, surpassing the limits never reached for synthetic Se-NPs.

As a future prospective for this first objective of the project, it would be beneficial to develop a more efficient purification process for the NPs, as they were difficult to isolate, remaining together with cellular debris. This prevented the use of higher concentrations of bacteria in the synthesis, which would have allowed a higher NP yield. This purification could be based on dialysis with a membrane pore size similar to the NP diameter. This membrane would remain in distilled water with continuous stirring until the NPs reached the solution (*Figure 25*).

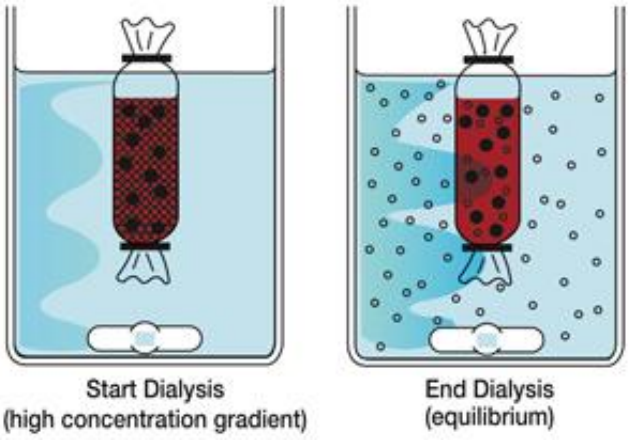

Figure 25. Fundamentals of Dialysis. Image from http://spectrumlabs.com/dialysis/Fund.html

Second, in order to gain a better understanding of the NP-bacteria interaction, a deeper study of the composition of the natural coating would be needed. This coating directly interacts with the bacterium, and differences in the proportion of the coating may vary the antimicrobial activity. Infrared spectroscopy studies would give an insight into the functional groups present in each of them. Moreover, theoretical simulation to make predictions of the interaction of these functional groups with the bacterial cell membrane would be useful to understand their mechanisms.

Finally, it would be interesting to try to obtain NPs enriched in the second metal, Cd, as the Cd/Se proportion in the ones synthesized was very low. This would give us an understanding of how the different proportion of both metals can affect their properties. To achieve this aim, it would be possible to genetically modify the bacteria. A resistant trait could be induced into the bacteria in order to express enzymes able to deal with the toxicity induced by the Cd ions by reducing them to produce NPs. In this way, the proportion of Cd could be increased in the NP and their possible different properties studied compared to their monometallic counterparts.

4.2. <u>Objective II</u>: Synthesis of Se-NPs by *H. pylori* to develop a novel route to treat its infection.

In the second objective of the project, the synthesis of Se-NPs by *H. pylori* was achieved for the first time to our knowledge, together with antimicrobial studies against the same bacteria that create them and *in vitro* cytotoxicity assays for HDF cells.

First, the ability of *H. pylori* to reduce selenite oxyanions from different metallic salts into Se-NPs was demonstrated. Though successful for selenite oxyanions, it should be noted that this bacterium was not able to reduce selenate oxyanions into elemental selenium. The metallic salt and its concentration was optimized in order to produce NPs in a high yield. Four different selenium metallic salts at seven concentrations were tested in order to achieve the best conditions. Sodium selenite at concentrations of 1, 2 and 5 mM produced the best impact on bacterial growth in comparison with the rest, thus they were selected for synthesis. Therefore, three different types of NPs were obtained: 1-SeNPs, 2-SeNPs and 5-SeNPs, corresponding to the initial concentration of Na_2SeO_3 used in the synthesis (1, 2, and 5 mM, respectively).

All NPs synthesized were characterized, showing equal morphologies and similar diameters. A higher metallic salt concentration produced more negatively charged NPs; thus, 5-SeNPs remained more stable in solution than the lower two concentrations. Additionally, the selenium composition of the metal NPs was validated by XPS studies.

Antimicrobial studies for the three types of Se-NPs at six different concentrations were carried out against *H. pylori*. From the bacterial growth curve assays, it could be inferred that 5-SeNPs showed the highest activity against bacteria. Moreover, the study of the biological parameters obtained by the modified Gompertz modeling gave insights into the effect of each concentration in bacterial growth. By analyzing the maximum value of the growth curve, the maximum exponential growth

rate and the lag time, 25 μg/mL was determined to be the optimal concentration of 5-SeNPs to treat the studied bacterium.

Because 5-SeNPs showed the best antibacterial activity of the three types of NPs, CFU assays were performed for five different concentrations of 5-SeNPs against *H. pylori*. Antimicrobial activity was exhibited for all the concentrations tested; however, only 10 μg/mL had significant activity against bacteria compared to the control. Thus, from these two assays it can be inferred that the most suitable concentrations of 5-SeNPs to treat *H. pylori* would be 10 and 25 μg/mL.

Finally, *in vitro* cytotoxicity studies were performed for HDF cells for 5-SeNPs at 5 different concentrations for 1, 3 and 5 days. The results showed that the only concentration that could be considered biocompatible for these cells was 5 μg/mL; however, concentrations of 10 μg/mL did not show cytotoxic effects before 24 h. As it was previously stated, most antibacterial treatments require approximately up to 8 h for both an efficient action and excretion through the urine, thus not being necessary to stay in contact with the human system for more than 24 h. Although the inherent nature of antibiotics and NPs differs one from each other, some parameters of the NPs could be controlled to induce their rapid clearance from the body. Aspects such as surface adsorption and size could be tailored to facilitate their excretion.

For future prospectives for this second objective of the project, first, the biocompatibility of the bacteriogenic Se-NPs should be improved for their implementation in biomedicine. As it was previously stated, the development of a more efficient purification process, via ultrasonication or more intense chemical washes, might remove part of the coating, thus reducing its pathogenic activity to a controllable level.

Second, it would be worth studying the cytotoxic effects of the synthesized NPs in epithelial cells, which are the ones present in the stomach wall, where *H. pylori* develops its pathogenic activity.

The studies developed in the project were in HDF cells, as they remain the standard healthy cells for biocompatibility studies in the laboratory.

Third, in order to study the possible resistance of the bacterium to the NPs, it would be possible to incubate them in presence of the NPs for different periods of time, and then, test the susceptibility to the NPs of the bacterium incubated with NPs compared to the normal strain. These time periods are left to allow the bacterium to develop a possible mutation against the NPs with which it is incubated.

Lastly, the acidic environment in the stomach to which the NPs would be exposed must be considered when trying to treat this bacterium. Therefore, the study of the behavior of the NPs at these exact conditions must be performed to ensure a good stability of the NPs in the stomach. The stomach wall is intrinsically covered by a thick coating of bicarbonate-rich mucus that blocks gastric juice from penetrating the underlying tissue layers. Thus, in case the NPs degrade in the stomach conditions, taking a biomimetic approach in which the NPs would be coated with bicarbonate groups on the surface in order to avoid acidic degradation, would be appealing to this project.

5. REFERENCES

[1] Hospital-Acquired Infection: Definition and Patient Education https://www.healthline.com/health/hospital-acquired-nosocomial-infections (accessed May 15, 2018).

[2] Woodford, N.; Ellington, M. J. The Emergence of Antibiotic Resistance by Mutation. Clin. Microbiol. Infect. 2007, 13 (1), 5–18.

[3] Antibiotics. Paediatr. Child Health 1999, 4 (7), 504.

[4] Origin of Bacterial Resistance to Antibiotics. Demerec M. Journal of bacteriology. 1948 vol: 56 (1) pp: 63-74

[5] Ventola, C. L. The Antibiotic Resistance Crisis: Part 1: Causes and Threats. *P T* 2015, *40* (4), 277–283.

[6] Antibiotics and bacterial resistance in the 21st century.Fair R, Tor Y. Perspectives in medicinal chemistry. 2014 vol: 6 pp: 25-64

[7] What Is MRSA Infection? Pictures, Symptoms, Treatment & Causes

[8] Methicillin-resistant Staphylococcus aureus (MRSA) Infections | MRSA | CDC https://www.cdc.gov/mrsa/index.html (accessed Jul 5, 2018).

[9] WHO | Antimicrobial Resistance. WHO 2018.

[10] Abat, C.; Rolain, J.-M.; Dubourg, G.; Fournier, P.-E.; Chaudet, H.; Raoult, D. Evaluating the Clinical Burden and Mortality Attributable to Antibiotic Resistance: The Disparity of Empirical Data and Simple Model Estimations. *Clin. Infect. Dis.* 2017, *65* (suppl_1), S58–S63.

[11] Das, B.; Patra, S. Antimicrobials. In *Nanostructures for Antimicrobial Therapy*; Elsevier, 2017; pp 1–22.Xiu, Z.; Zhang, Q.; Puppala, H. L.; Colvin, V. L.; Alvarez, P.

J. J. Negligible Particle-Specific Antibacterial Activity of Silver Nanoparticles. *Nano Lett.* 2012, *12* (8), 4271–4275.

[12] Petros, R. A.; DeSimone, J. M. Strategies in the Design of Nanoparticles for Therapeutic Applications. *Nat. Rev. Drug Discov.* 2010, *9* (8), 615–627.

[13] Khan, I.; Saeed, K.; Khan, I. Nanoparticles: Properties, Applications and Toxicities. *Arab. J. Chem.* 2017.

[14] Salata, O. Applications of Nanoparticles in Biology and Medicine. *J. Nanobiotechnology* 2004, *2* (1), 3.

[15] Parveen, S.; Misra, R.; Sahoo, S. K. Nanoparticles: A Boon to Drug Delivery, Therapeutics, Diagnostics and Imaging. *Nanomedicine Nanotechnology, Biol. Med.* 2012, 8 (2), 147–166.

[16] Davis, M. E.; Chen, Z.; Shin, D. M. Nanoparticle Therapeutics: An Emerging Treatment Modality for Cancer. Nat. Rev. Drug Discov. 2008, 7 (9), 771–782.

[17] Mesoporous silica nanoparticles as a delivery system for hydrophobic anticancer drugs. Lu J, Liong M, Zink JI, Tamanoi F. Small. 2007 Aug; 3(8):1341-6.

[18] Abd Ellah, N. H.; Abouelmagd, S. A. Surface Functionalization of Polymeric Nanoparticles for Tumor Drug Delivery: Approaches and Challenges. Expert Opin. Drug Deliv. 2017, 14 (2), 201–214.

[19] Tian J, Wong KK, Ho CM, Lok CN, Yu WY, Che CM, Chiu JF, Tam PK. Topical delivery of silver nanoparticles promotes wound healing. ChemMedChem 2007, 2:129–136.

[20] Yamada, M.; Foote, M.; Prow, T. W. Therapeutic Gold, Silver, and Platinum Nanoparticles. *WIREs Nanomed Nanobiotechnol* 2015, *7*, 428–445.

[21] Wernicki, Andrzej & Puchalski, Andrzej & Urban-Chmiel, Renata & Dec, Marta & Stęgierska, D & Nowaczek, Anna & Wojcik, Anna. (2014). Antimicrobial properties of gold, silver, copper and platinum nanoparticles against selected microorganisms isolated from cases of mastitis in cattle. Medycyna Weterynaryjna. 70. 564-567.

[22] Metal nanoparticles: understanding the mechanisms behind antibacterial activity. Slavin Y , Asnis J, Häfeli U, Bach H. Journal of Nanobiotechnology. 2017 vol: 15 (1) pp: 65

[23] Rajeshkumar, S. Anticancer Activity of Eco-Friendly Gold Nanoparticles against Lung and Liver Cancer Cells. *J. Genet. Eng. Biotechnol.* 2016, *14* (1), 195–202.

[24] Hajipour, M. J.; Fromm, K. M.; Akbar Ashkarran, A.; Jimenez de Aberasturi, D.; Larramendi, I. R. de; Rojo, T.; Serpooshan, V.; Parak, W. J.; Mahmoudi, M. Antibacterial Properties of Nanoparticles. *Trends Biotechnol.* 2012, *30* (10), 499–511.

[25] Jain, J.; Arora, S.; Rajwade, J. M.; Omray, P.; Khandelwal, S.; Paknikar, K. M. Silver Nanoparticles in Therapeutics: Development of an Antimicrobial Gel Formulation for Topical Use. *Mol. Pharm.* 2009, *6* (5), 1388–1401.

[26] Wei, L.; Lu, J.; Xu, H.; Patel, A.; Chen, Z.-S.; Chen, G. Silver Nanoparticles: Synthesis, Properties, and Therapeutic Applications. *Drug Discov. Today* 2015, *20* (5), 595–601.

[27] Hornos Carneiro, M. F.; Barbosa, F. Gold Nanoparticles: A Critical Review of Therapeutic Applications and Toxicological Aspects. *J. Toxicol. Environ. Heal. Part B* 2016, *19* (3–4), 129–148.

[28] Fujiwara, R.; Luo, Y.; Sasaki, T.; Fujii, K.; Ohmori, H.; Kuniyasu, H. Cancer Therapeutic Effects of Titanium Dioxide Nanoparticles Are Associated with Oxidative Stress and Cytokine Induction. *Pathobiology* 2015, *82* (6), 243–251.

[29] Rathod, T.; Padalia, H.; Chanda, S. Green Synthesized Zinc Oxide Nanoparticles as a Therapeutic Tool to Combat Candidiasis. In *AIP Conference Proceedings*; AIP Publishing LLC , 2017; Vol. 1837, p 40065.

[30] Antimicrobial activity of iron oxide nanoparticle upon modulation of nanoparticle-bacteria interface. Arakha M, Pal S, Samantarrai D, Panigrahi T, Mallick B et. al. Scientific Reports. 2015 vol: 5 (1) pp: 1481.

[31] Luo, G.-F.; Chen, W.-H.; Liu, Y.; Lei, Q.; Zhuo, R.-X.; Zhang, X.-Z. Multifunctional Enveloped Mesoporous Silica Nanoparticles for Subcellular Co-Delivery of Drug and Therapeutic Peptide. *Sci. Rep.* 2015, *4* (1), 6064.

[32] Chen, Z.; Zhang, A.; Wang, X.; Zhu, J.; Fan, Y.; Yu, H.; Yang, Z. The Advances of Carbon Nanotubes in Cancer Diagnostics and Therapeutics. *J. Nanomater*. 2017, *2017*, 1–13.

[33] Yun, Y. Carbon Nanomaterials: From Therapeutics to Regenerative Medicine. *J. Nanomedine. Biotherapeutic Discov.* 2012, *2* (1).

[34] Akram Raza, M.; Kanwal, Z.; Rauf, A.; Sabri, A. N.; Riaz, S.; Naseem, S. Size-and Shape-Dependent Antibacterial Studies of Silver Nanoparticles Synthesized by Wet Chemical Routes.

[35] Singh, A. K.; Singh, P.; Srivastava, A. Antibacterial Fe3O4 Nanoparticles: Synthesis and Characterization. J. Eng. Res. Appl. www.ijera.com ISSN 2017, 7 (85), 2248–962232.

[36] Reddy, L. S.; Nisha, M. M.; Joice, M.; Shilpa, P. N. Antimicrobial Activity of Zinc Oxide (ZnO) Nanoparticle against Klebsiella Pneumoniae. Pezzuto Pharm Biol 2014, 52 (11), 1388–1397.

[37] Mechanisms of nanotoxicity: Generation of reactive oxygen species. Xia Q, Hwang H, Ray P, Yu H. Journal of Food and Drug Analysis. 2014 vol: 22 (1) pp: 64-75

[38] Chakrabarti, P. Interaction of Metal Ions with Carboxylic and Carboxamide Groups in Protein Structures. Protein Eng. 1990, 4 (1), 49–56.

[39] Synthesis of Nanoparticles by Laser Ablation: A Review. Kim M, Osone S, Kim T, Higashi H, Seto T. KONA Powder and Particle Journal. 2017 vol: 34 (0) pp: 80-90

[40] UV-induced synthesis, characterization and formation mechanism of silver nanoparticles in alkalic carboxymethylated chitosan solution. Huang L, Zhai M, Long D, Peng J, Xu L et. Al. Journal of Nanoparticle Research. 2008 vol: 10 (7) pp: 1193-1202

[41] Hydrothermal Synthesis of Metal Oxide Nanoparticles in Supercritical Water. Hayashi H, Hakuta Y. Materials. 2010 vol: 3 (7) pp: 3794-3817

[42] Dhand, C.; Dwivedi, N.; Loh, X. J.; Ng, A.; Ying, J.; Verma, N. K.; Beuerman, R. W.; Lakshminarayanan, R.; Ramakrishna, S. Methods and Strategies for the Synthesis of Diverse Nanoparticles and Their Applications: A Comprehensive Overview.

[43] Synthesis of silver nanoparticles by chemical and biological methods and their antimicrobial properties. Gudikandula K, Charya Maringanti S. Journal of Experimental Nanoscience. 2016 vol: 11 (9) pp: 714-721

[44] Shape and Aggregation Control of Nanoparticles: Not Shaken, Not Stirred. Li D, Kaner R.

[45] Stealth Biocompatible Si-Based Nanoparticles for Biomedical Applications. Liu W, Chaix A, Gary-Bobo M, Angeletti B, Mason A et. Al. Nanomaterials. 2017 vol: 7 (10) pp: 288

[46] Green chemistry. Royal Society of Chemistry (Great Britain) Publisher: Royal Society of Chemistry. 1999

[47] G. Ingale, A.; Chaudhari, A. N. Biogenic Synthesis of Nanoparticles and Potential Applications: An Eco- Friendly Approach. *J. Nanomed. Nanotechnol.* 2013, *4* (2), 1–8.

[48] Green chemistry for nanoparticle synthesis. Duan H, Wang D, Li Y. Chemical Society Reviews. 2015 vol: 44 (16) pp: 5778-5792

[49] Bacteriogenic synthesis of selenium nanoparticles by Escherichia coli ATCC 35218 and its structural characterization. Kora A, Rastogi L. IET Nanobiotechnology. 2017 vol: 11 (2) pp: 179-184

[50] Bacterial resistance and detoxification of heavy metals. Williams J, Silver S. Enzyme and Microbial Technology Volume 6, Issue 12, December 1984, Pages 530-537

[51] Medina Cruz, D.; Mi, G.; Webster, T. J. Synthesis and Characterization of Biogenic Selenium Nanoparticles with Antimicrobial Properties Made by *Staphylococcus Aureus*, Methicillin-Resistant *Staphylococcus Aureus* (MRSA), *Escherichia Coli*, and *Pseudomonas Aeruginosa*. *J. Biomed. Mater. Res. Part A* 2018, *106* (5), 1400–1412.

[52] Iravani, S. Bacteria in Nanoparticle Synthesis: Current Status and Future Prospects. *Int. Sch. Res. Not.* 2014, *2014*, 1–18.

[53] Klaus-Joerger, T.; Joerger, R.; Olsson, E.; Granqvist, C.-G. Bacteria as Workers in the Living Factory: Metal-Accumulating Bacteria and Their Potential for Materials Science. *Trends Biotechnol.* 2001, *19* (1), 15–20.

[54] He, S.; Guo, Z.; Zhang, Y.; Zhang, S.; Wang, J.; Gu, N. Biosynthesis of Gold Nanoparticles Using the Bacteria Rhodopseudomonas Capsulata. *Mater. Lett.* 2007, *61* (18), 3984–3987.

[55] Gerrard T, Telford J, Williams H. Detection of selenium deposits in Escherichia coli by electron microscopy. J Bacteriol 1974;119: 1057–1060

[56] Kessi J, Ramuz M, Wehrli E, Spycher M, Bachofen R. Reduction of selenite and detoxification of elemental selenium by the phototrophic bacterium Rhodospirillum rubrum. Appl Environ Microbiol 1999 ; 65:4734–4740.

[57] Nancharaiah, Y. V; Lens, P. N. L. Ecology and Biotechnology of Selenium-Respiring Bacteria. Microbiol. Mol. Biol. Rev. 2015, 79 (1), 61–80.

[58] Li, D.-B.; Cheng, Y.-Y.; Wu, C.; Li, W.-W.; Li, N.; Yang, Z.-C.; Tong, Z.-H.; Yu, H.-Q. Selenite Reduction by Shewanella Oneidensis MR-1 Is Mediated by Fumarate Reductase in Periplasm. Sci. Rep. 2014, 4, 3735.

[59] Samiran Mondal, Nayan Roy, Rajibul A. Laskar, Ismail Sk, Saswati Basu, Debabrata Mandal, Naznin Ara Begum, Biogenic synthesis of Ag, Au and bimetallic Au/Ag alloy nanoparticles using aqueous extract of mahogany (Swietenia mahogani JACQ.) leaves, Colloids and Surfaces B: Biointerfaces, Volume 82, Issue 2, 2011, Pages 497-504

[60] Renata Dobrucka, Jolanta Dlugaszewska, Antimicrobial activity of the biogenically synthesized core-shell Cu@Pt nanoparticles, Saudi Pharmaceutical Journal, Volume 26, Issue 5, 2018, Pages 643-650

[61] Deepak Kumar Gupta, Mahesh Verma, Dinesh Patidar, Kananbala Sharma and N. S. Saxena. Nanoscience & Nanotechnology-Asia (2017) 7: 73.

[62] Kumar, P. Vijaya. (2016). Synthesis and Characterization of ZnSe Nanoparticles by Co-precipitation Method. Journal of Nanoscience and Technology. 2. 148-150.

[63] Aeshah Salem, Elias Saion, Naif Mohammed Al-Hada, Halimah Mohamed Kamari, Abdul Halim Shaari, Shahidan Radiman,Simple synthesis of ZnSe nanoparticles by

thermal treatment and their characterization,Results in Physics, Volume 7, 2017,Pages 1175-1180

[64] Metz, K. M.; Sanders, S. E.; Pender, J. P.; Dix, M. R.; Hinds, D. T.; Quinn, S. J.; Ward, A. D.; Duffy, P.; Cullen, R. J.; Colavita, P. E. Green Synthesis of Metal Nanoparticles via Natural Extracts: The Biogenic Nanoparticle Corona and Its Effects on Reactivity. ACS Sustain. Chem. Eng. 2015, 3 (7), 1610–1617.

[65] Core@shell Nanoparticles: Greener Synthesis Using Natural Plant Products. Khatami M, Alijani H, Nejad M, Varma . Applied Sciences. 2018 vol: 8 (3) pp: 411

[66] Haefeli, C.; Franklin, C.; Hardy, K. Plasmid-Determined Silver Resistance in Pseudomonas Stutzeri Isolated from a Silver Mine. *J. Bacteriol.* 1984, *158* (1), 389–392.

[67] Luis F. Hakim, Julie L. Portman, Michelle D. Casper, Alan W. Weimer, Aggregation behavior of nanoparticles in fluidized beds, *Powder Technology*, Volume 160, Issue 3, 2005.

[68] Jeffrey W. Williams, Simon Silver, Bacterial resistance and detoxification of heavy metals, Enzyme and Microbial Technology, Volume 6, Issue 12, 1984, Pages 530-537. ISSN 0141-0229

[69] Kaakoush, N. O.; Raftery, M.; Mendz, G. L. Molecular Responses of Campylobacter Jejuni to Cadmium Stress. FEBS J. 2008, 275 (20), 5021–5033.

[70] Halder, S.; Yadav, K. K.; Sarkar, R.; Mukherjee, S.; Saha, P.; Haldar, S.; Karmakar, S.; Sen, T. Alteration of Zeta Potential and Membrane Permeability in Bacteria: A Study with Cationic Agents. Springerplus 2015, 4, 672.

[71] Takashima S, Morisaki H (1997) Surface characteristics of the microbial cell of *Pseudomonas syringae* and its relevance to cell attachment. Colloids Surf B Biointerfaces 9:205–212

[72] Scholl MA, Harvey RW (1992) Laboratory investigations on the role of sediment surfaces and ground water chemistry in transport of bacteria through a contaminated sandy aquifer. Environ Sci Technol 26:1410–1417

[73] Yongsuk H, Brown DG (2006) Cell surface acid–base properties of Escherichia coli and Bacillus brevis and variation as a function of growth phase, nitrogen source and C:N ratio. Colloids Surf B Biointerfaces 50:112–119

[74] Size-, composition- and shape-dependent toxicological impact of metal oxide nanoparticles and carbon nanotubes toward bacteria. Simon-Deckers A, Loo S, Mayne-L'hermite M, Herlin-Boime N, Menguy N, Reynaud C, Gouget B, Carrière M. Environ Sci Technol. 2009 Nov 1; 43(21):8423-9.

[75] Why do Gram positive and Gram negative bacteria show different antibiotic susceptibility patterns? | AIMED - Let's talk about antibiotics https://aimed.net.au/2015/08/12/why-do-gram-positive-and-gram-negative-bacteria-show-different-antibiotic-susceptibility-patterns/ (accessed Jul 15, 2018).

[76] Trang H.D. Nguyen, Bongkosh Vardhanabhuti, Mengshi Lin, Azlin Mustapha, Antibacterial properties of selenium nanoparticles and their toxicity to Caco-2 cells, Food Control, Volume 77, 2017, Pages 17-24

[77] Mahsa, Y.; Hamed, A.; Amir, A. A. Antibacterial Activity of Silver-Nanoparticles against Staphylococcus Aureus. African J. Microbiol. Res. 2016, 10 (23), 850–855.

[78] Sun, Q.; Kanehira, K.; Taniguchi, A. Low Doses of TiO2 -Polyethylene Glycol Nanoparticles Stimulate Proliferation of Hepatocyte Cells. Sci. Technol. Adv. Mater. 2016, 17 (1), 669–676.

[79] Bhattacharjee, S. DLS and Zeta Potential – What They Are and What They Are Not? J. Control. Release 2016, 235, 337–351.

[80] Wai, S. N.; Mizunoe, Y.; Takade, A.; Yoshida, S. Arch. Microbiol. 2000, 173, 307−310.

[81] Cuny, C.; Lesbats, M. N.; Dukan, S. Appl. Environ. Microbiol. 2007, 73, 885−889.

[82] Wang, L.; Hu, C.; Shao, L. The Antimicrobial Activity of Nanoparticles: Present Situation and Prospects for the Future. Int. J. Nanomedicine 2017, 12, 1227–1249.